Measuring TeV Cosmic Rays at the HAWC Observatory

Segev BenZvi
Department of Physics and Astronomy
University of Rochester

HAWC Observatory

- The **H**igh **A**ltitude **W**ater **C**herenkov Gamma-ray Observatory (HAWC) is operating and nearly complete
- Goals: observe gamma rays and cosmic rays from half the sky each day between 100 GeV and 100 TeV
  - 4100 meters above sea level
  - 19°N latitude (Galactic Center at 48° zenith)
  - 300 water tanks, 1200 semi-hemispherical PMTs
  - 1/6th of sky in instantaneous field of view
- Current status: tank construction and water filtration completed, Jan. 15, final PMTs deploying. 250 tanks in DAQ

Detector Location

- Parque Nacional Pico de Orizaba: 97.5°W, 18.9°N

J L Macías, GSA Special Papers **422**:183, 2007

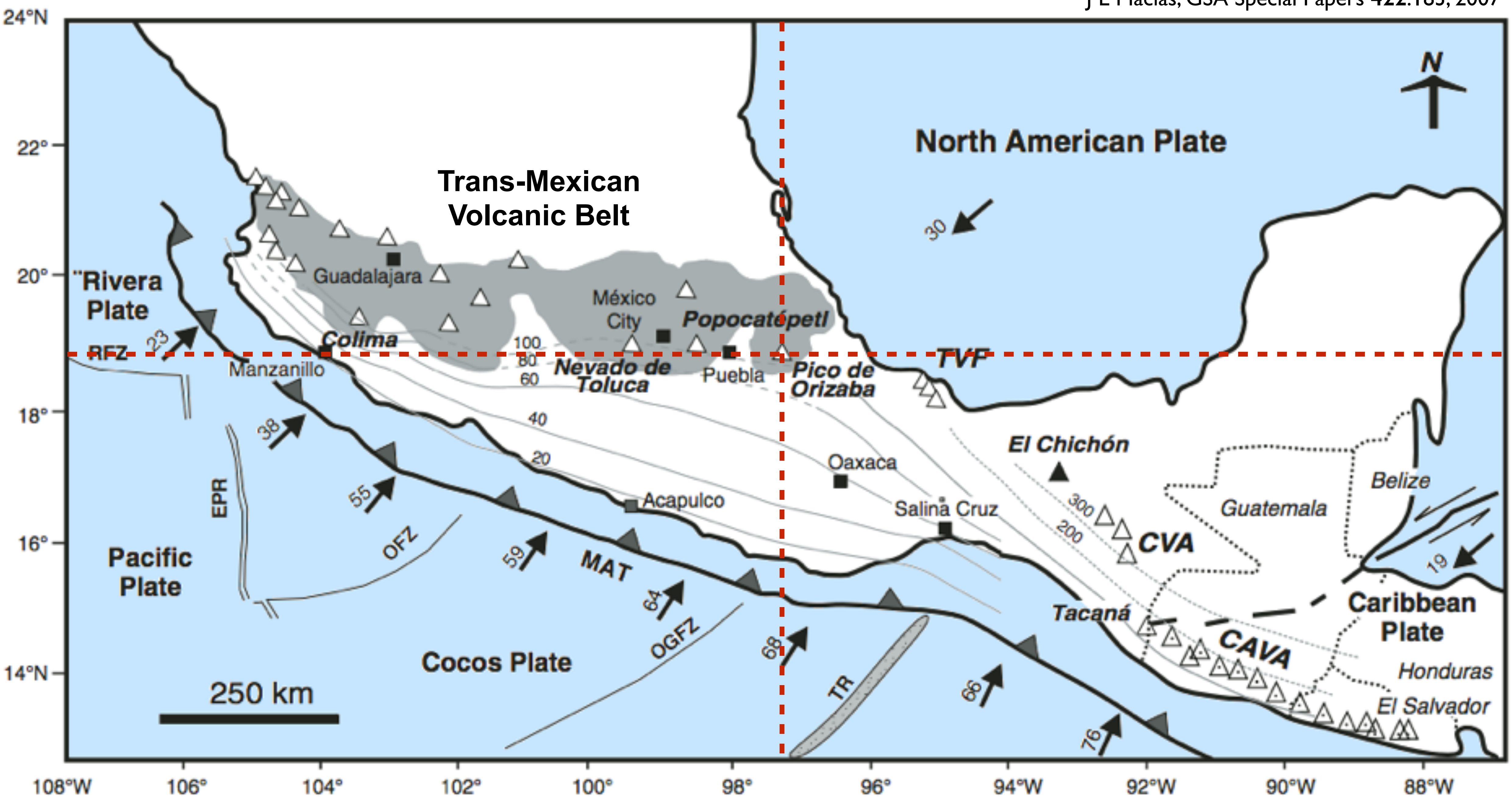

HAWC Site

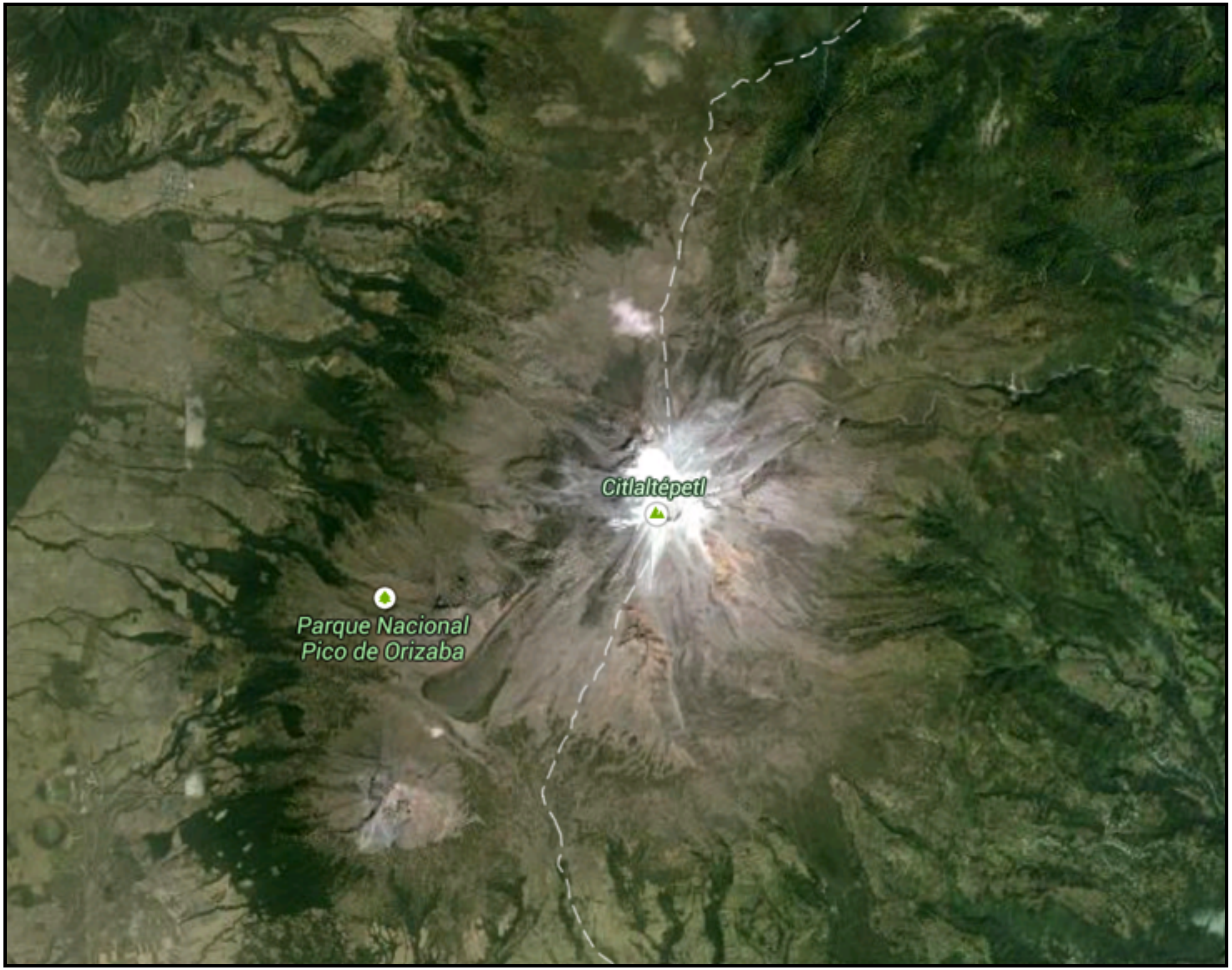

HAWC Site

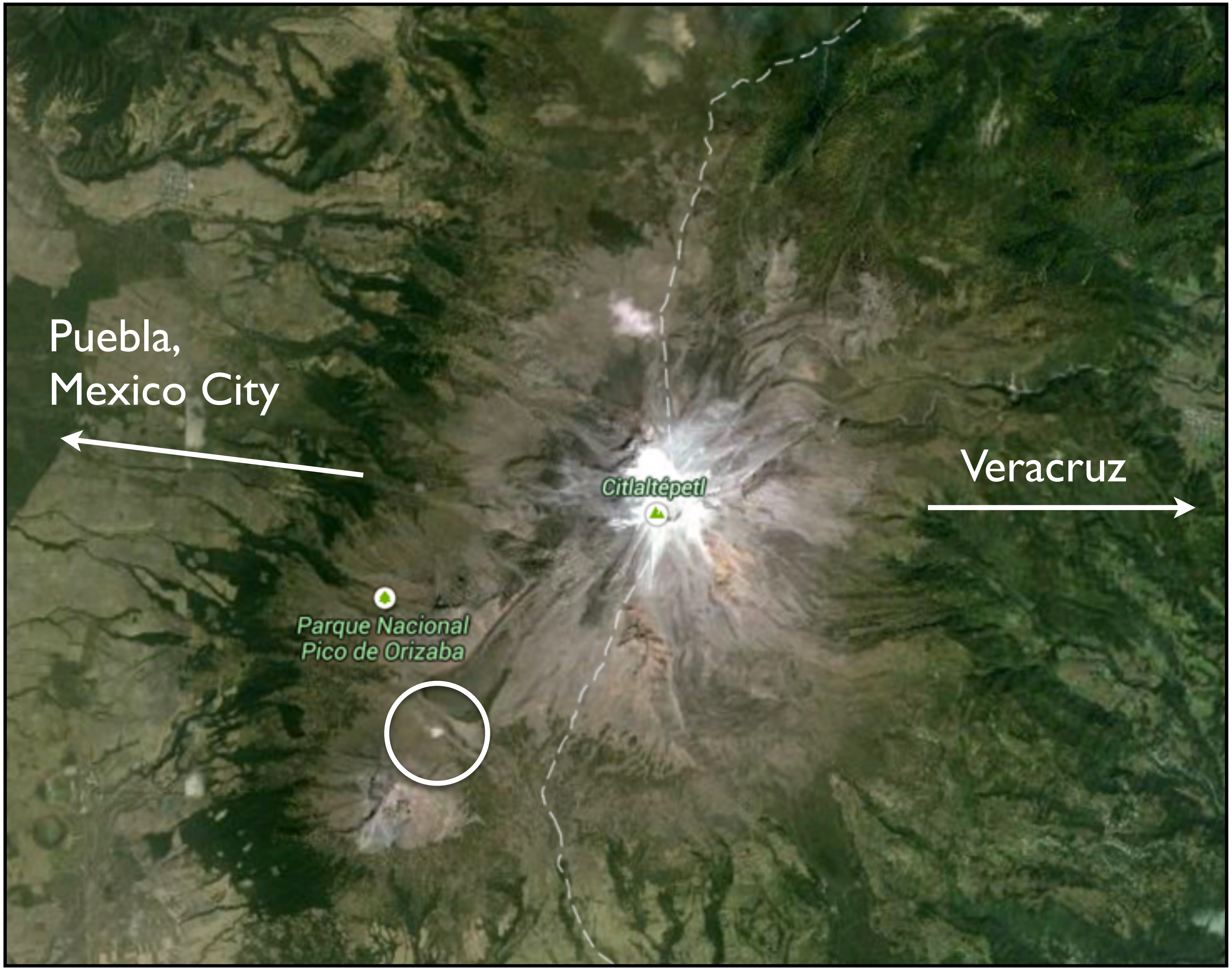

Puebla,
Mexico City
Veracruz
Citlaltépetl
Parque Nacional
Pico de Orizaba

HAWC Site

HAWC Site

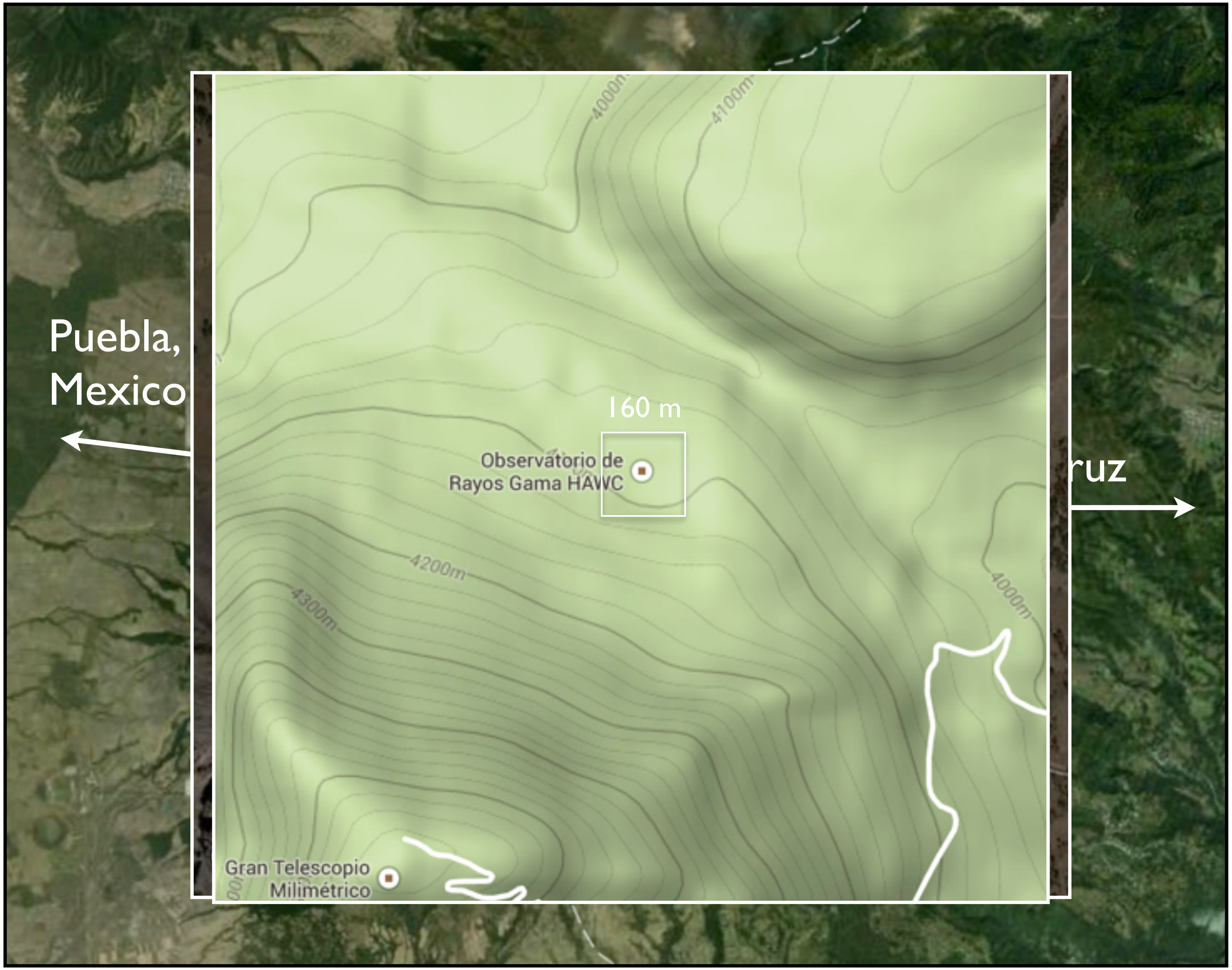
Puebla,
Mexico
ruz
160 m
Observatorio de
Rayos Gama HAWC
4000m
4100m
4200m
4300m
4000m
Gran Telescopio
Milimétrico

HAWC Site


Pico de Orizaba
("Citlaltepetl")
5636 meters
Lava flow
~60 meters
Platform
4100 meters
Sierra Negra
4582 meters

Water Cherenkov Method

- Robust and cost-effective surface detection technique
- Water tanks: 7.3 m radius, 5 m height, 185 kL purified water
- Tanks contain three 8” R5912 PMTs and one 10” R7081-HQE PMT looking up to capture Cherenkov light from shower front

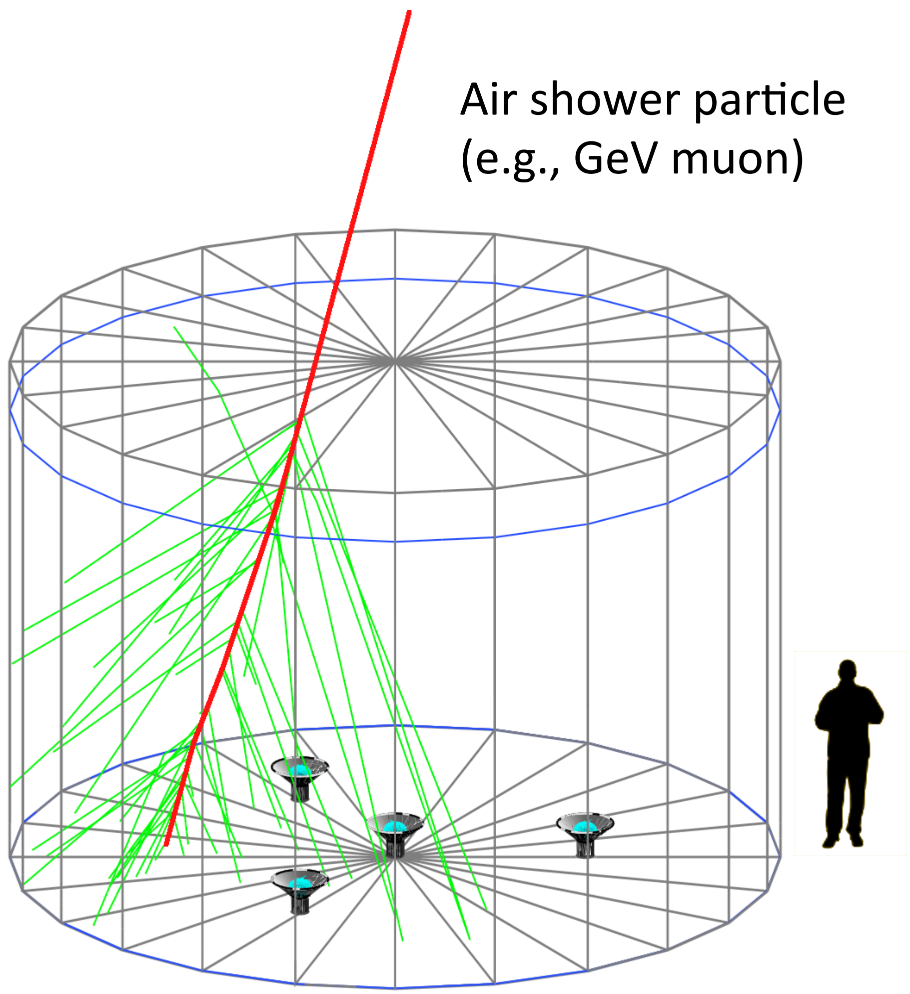

Tank Deployment

- Tanks built using 5 "rings" of curved steel panels; then capped with an opaque military-grade canvas roof

- Next step: bladder deployment, water delivery, and PMT deployment. Work: local crew of about 25 people

HAWC Detector

16 Jan 2015

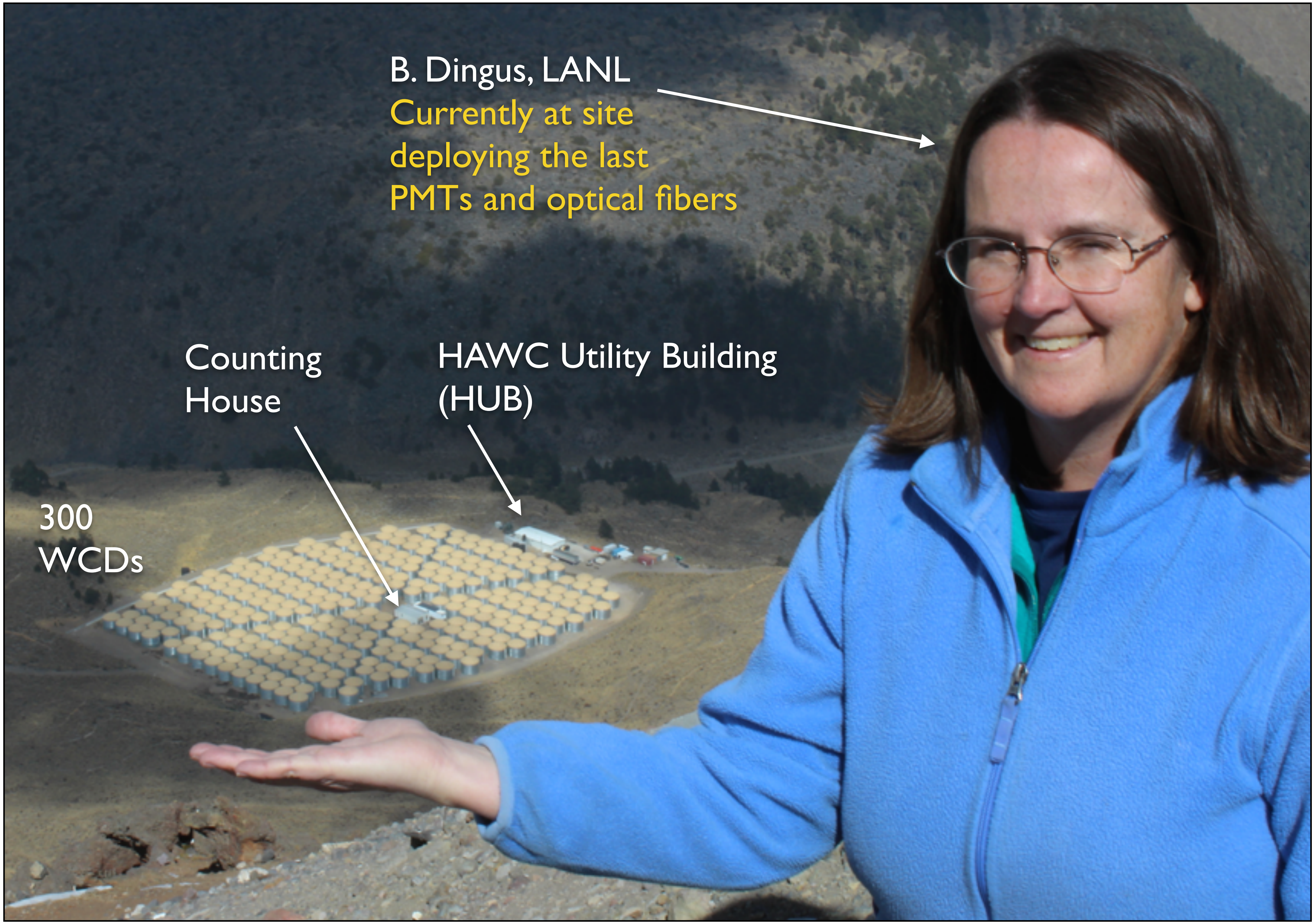

Detector: 55 kT of Water

Detector: 55 kT of Water

Cabling

- Buried coaxial cables used to connect PMTs to HV supply and front-end electronics in the Counting House

- Total length of cable used: 180 km

Signal Processing

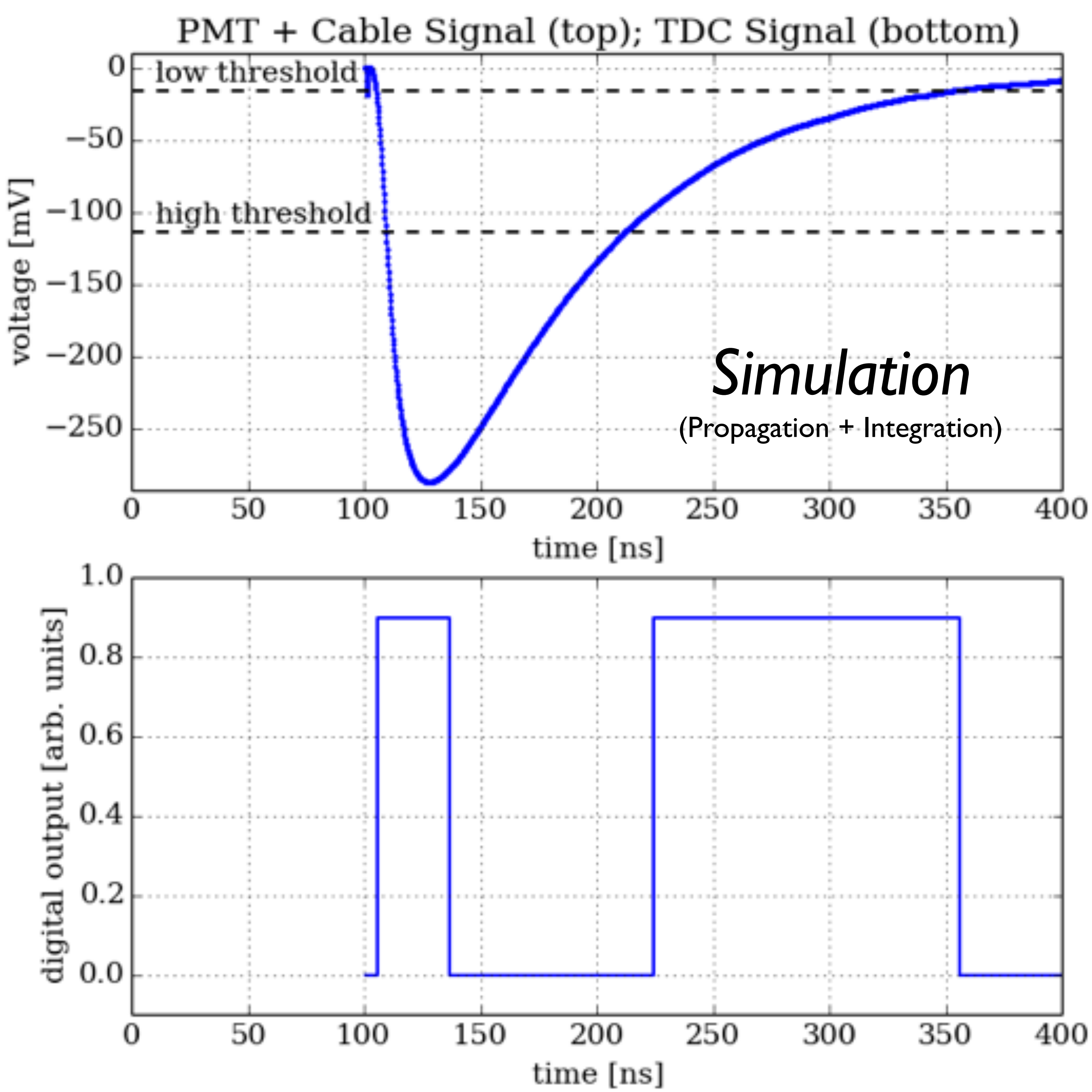

- Compression achieved using V1190 TDCs from CAEN
- PMT $V(t)$ → logic pulse with 2 or 4 "edge" transitions; 100 ps resolution per edge
- Charge-TOT absolute calibration performed at LANL. HV gain-matching during PMT deployment
- Detector drift: weekly laser shots, plus long-term water clarity measurements
- Rate from 1200 PMTs after TDC compression: 0.5 GB/s

Software Trigger

- A computing farm in the Counting House is used to apply a simple multiplicity trigger to the data in software. No topological cuts are applied at trigger level.

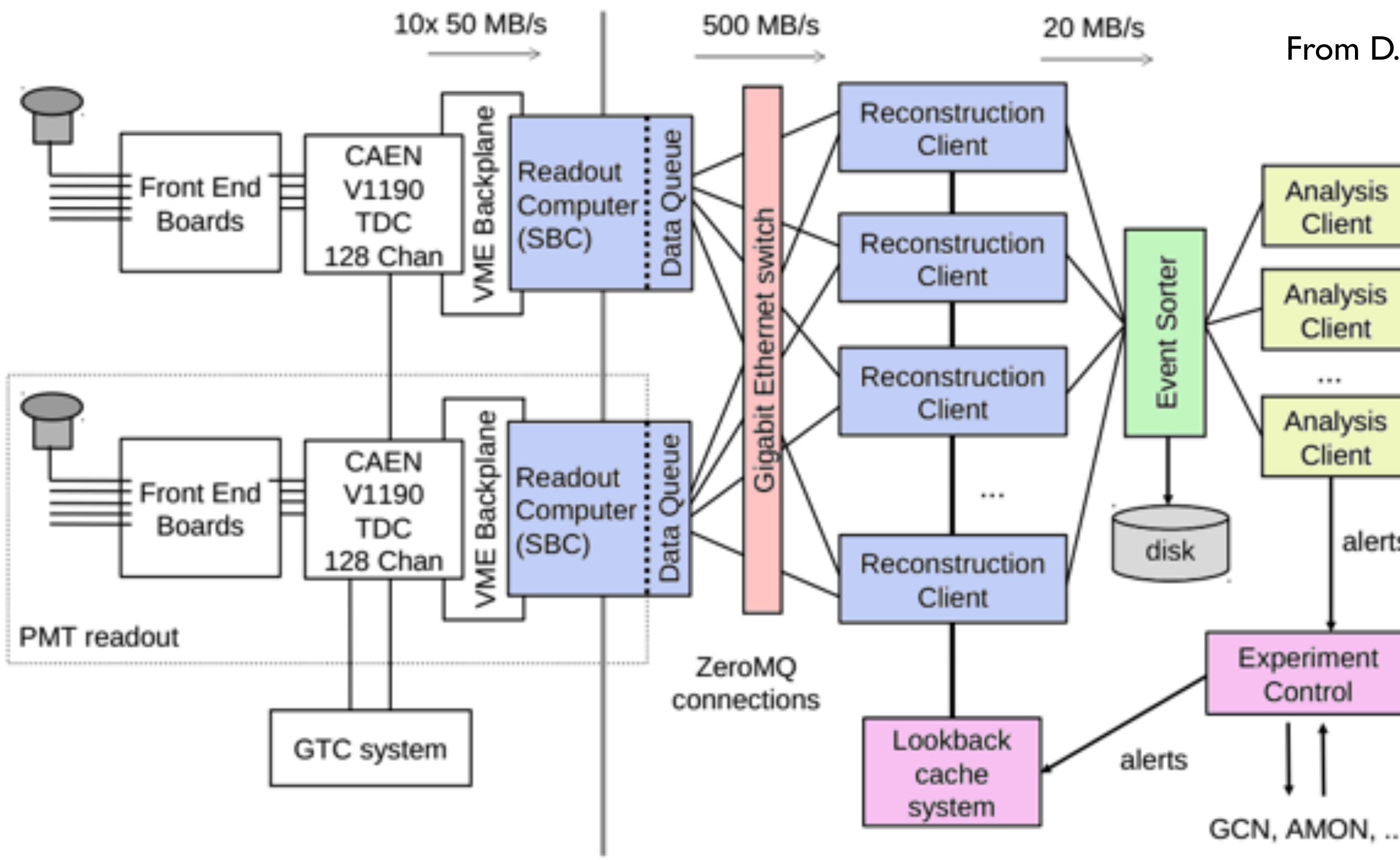

From D. Zaborov, G. Kunde, et al., in prep.

- After the the trigger, the event rate is reduced to 20 kHz, or a data rate of ~0.02 GB/s (2 TB/day)

Background Rejection

- CR rejection using topological cut in hit pattern

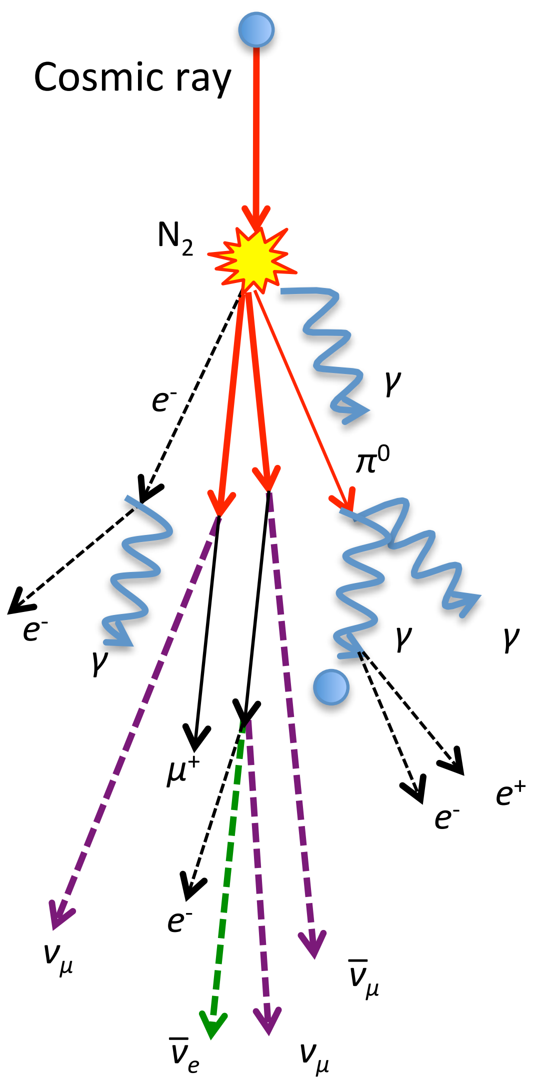

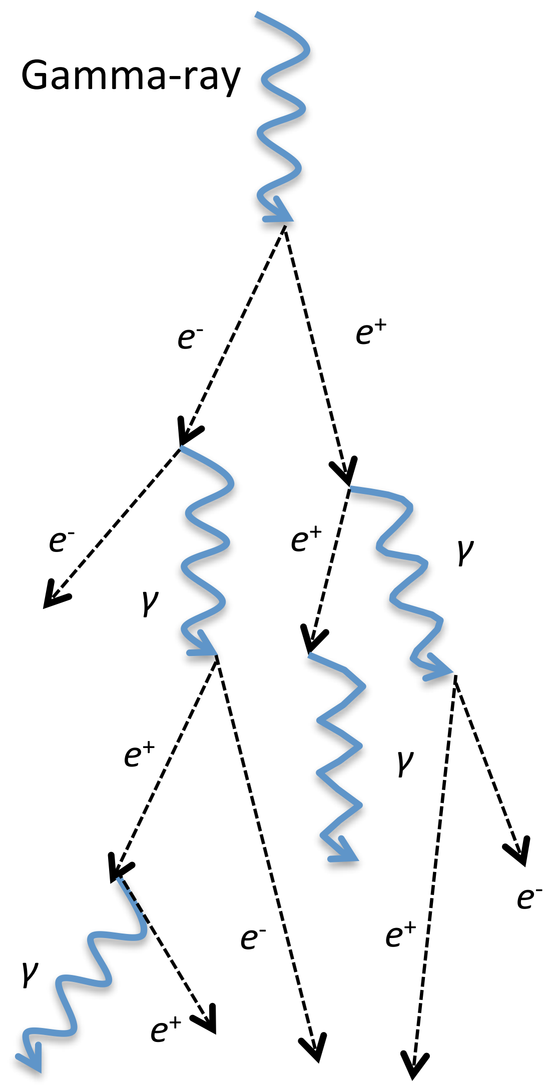

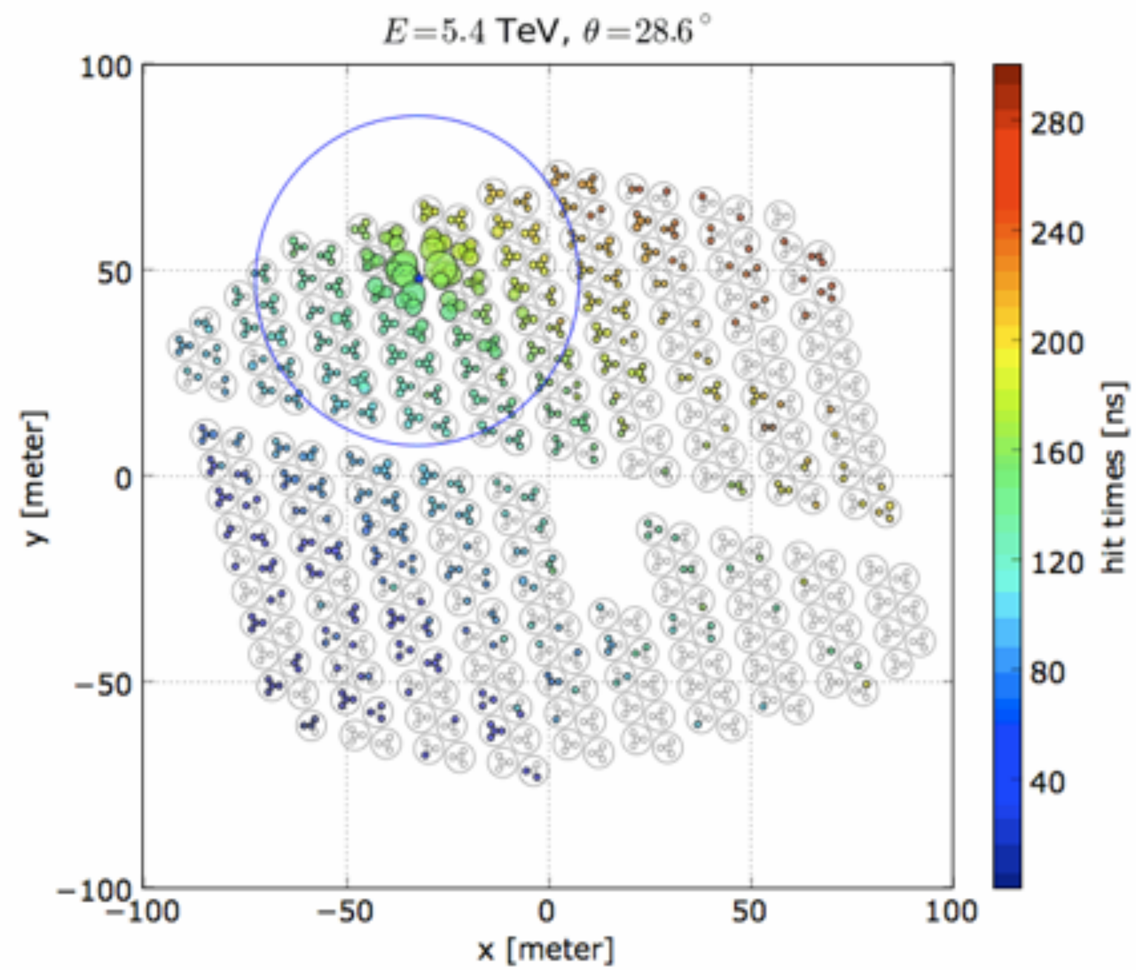

- Requires sufficient number of triggered channels (>70) to work well. Q-value ($\epsilon_\gamma/\sqrt{\epsilon_{CR}}$) is ~5 for point sources

Background Rejection

- CR rejection using topological cut in hit pattern

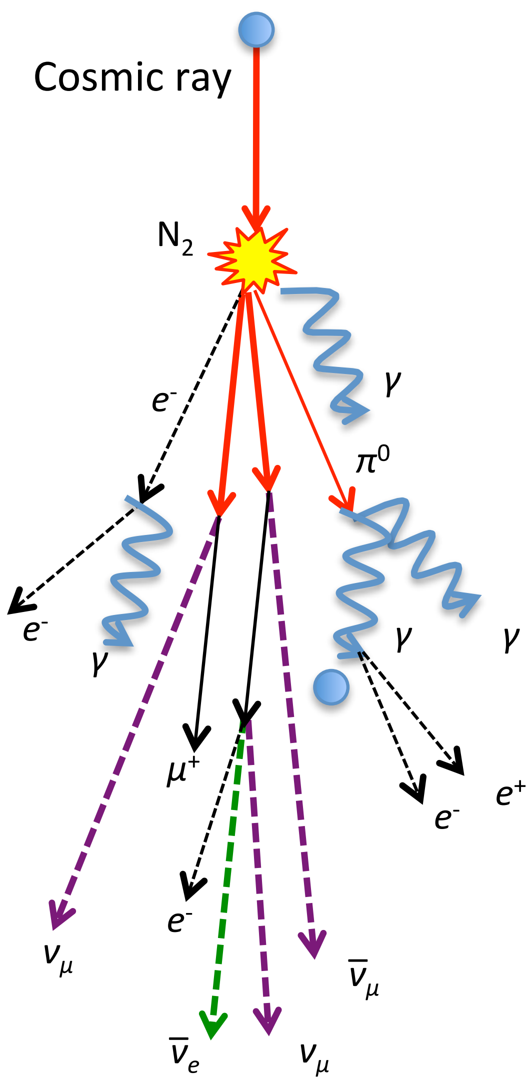

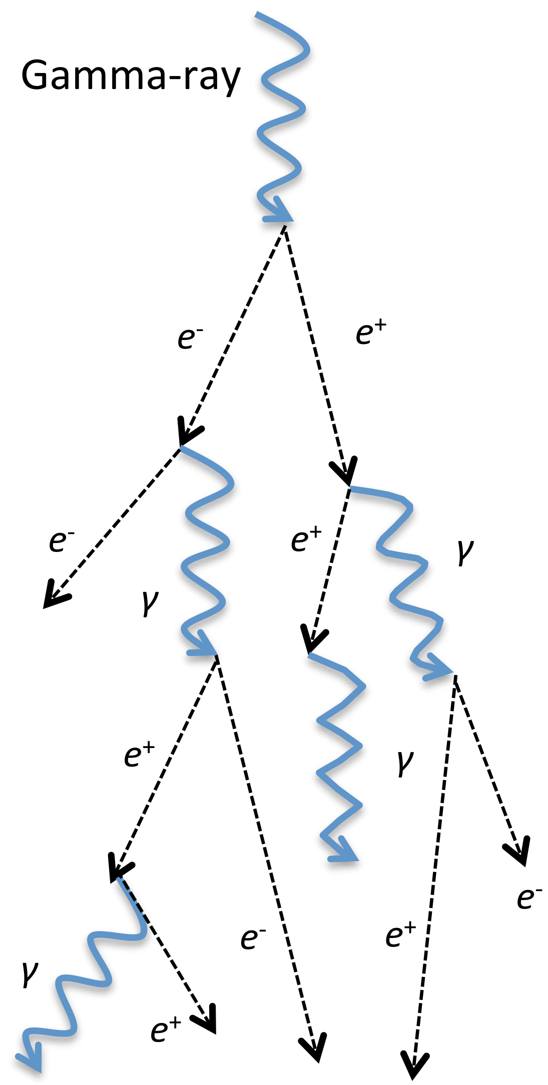

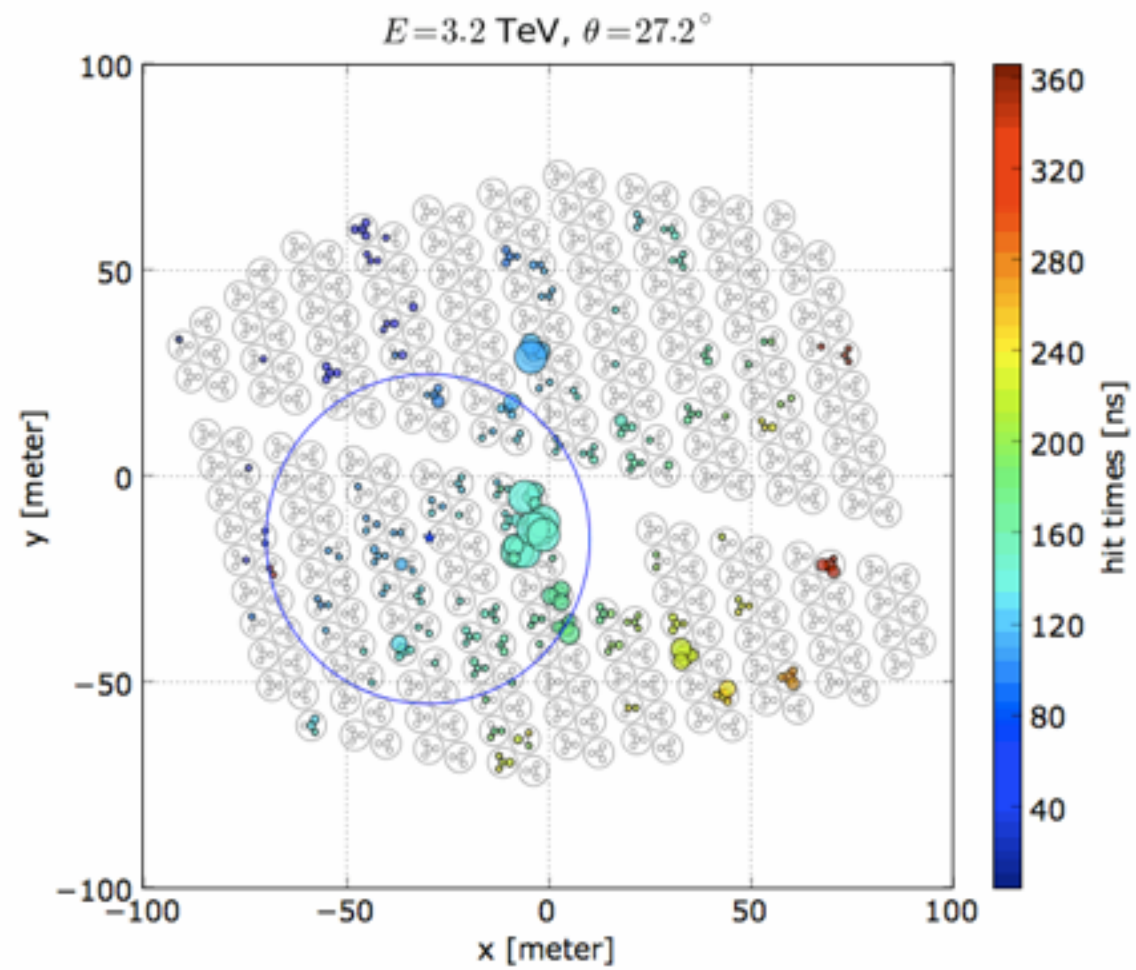

- Requires sufficient number of triggered channels (>70) to work well. Q-value ($\epsilon_\gamma/\sqrt{\epsilon_{CR}}$) is ~5 for point sources

HAWC-250 Event

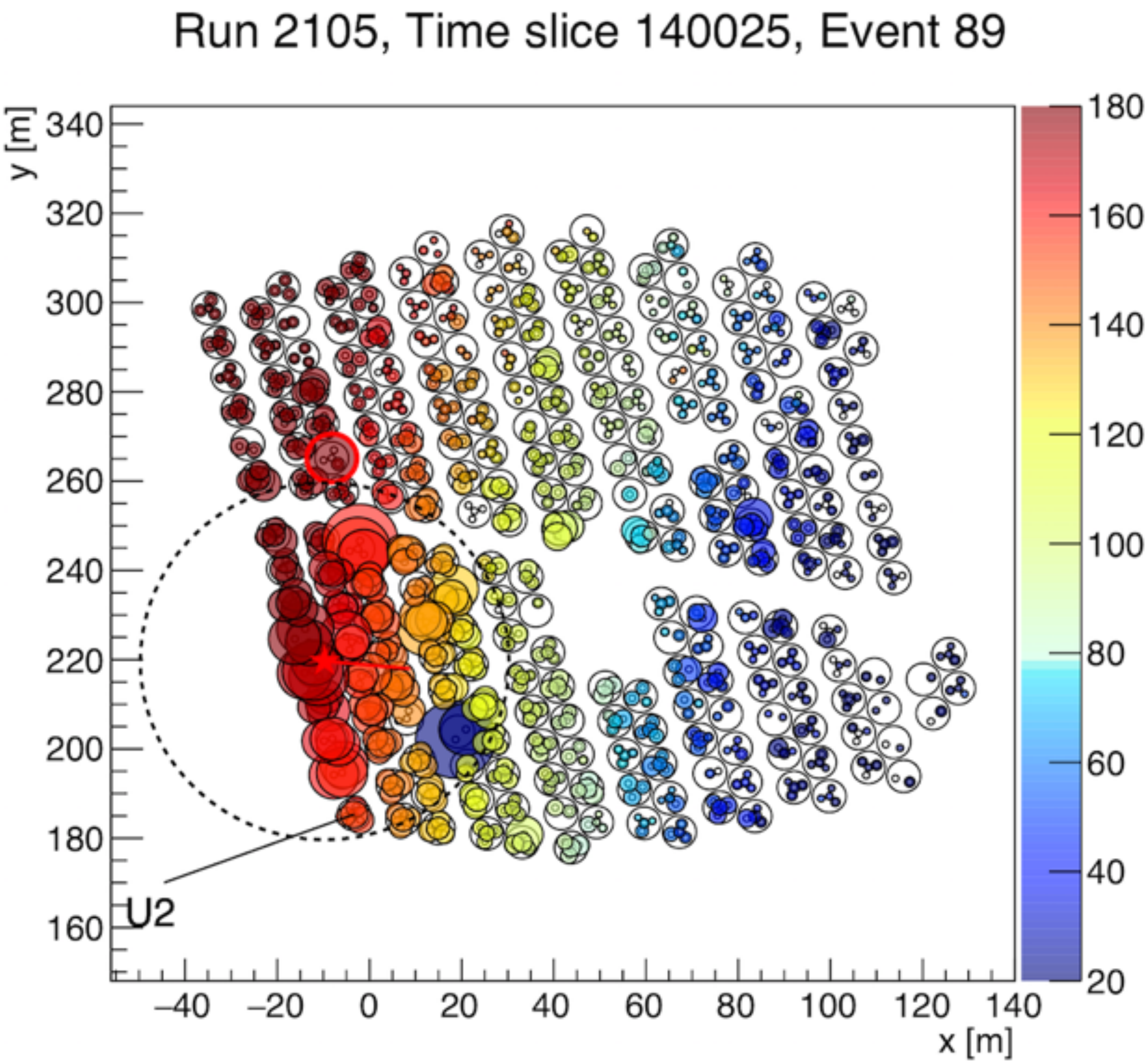

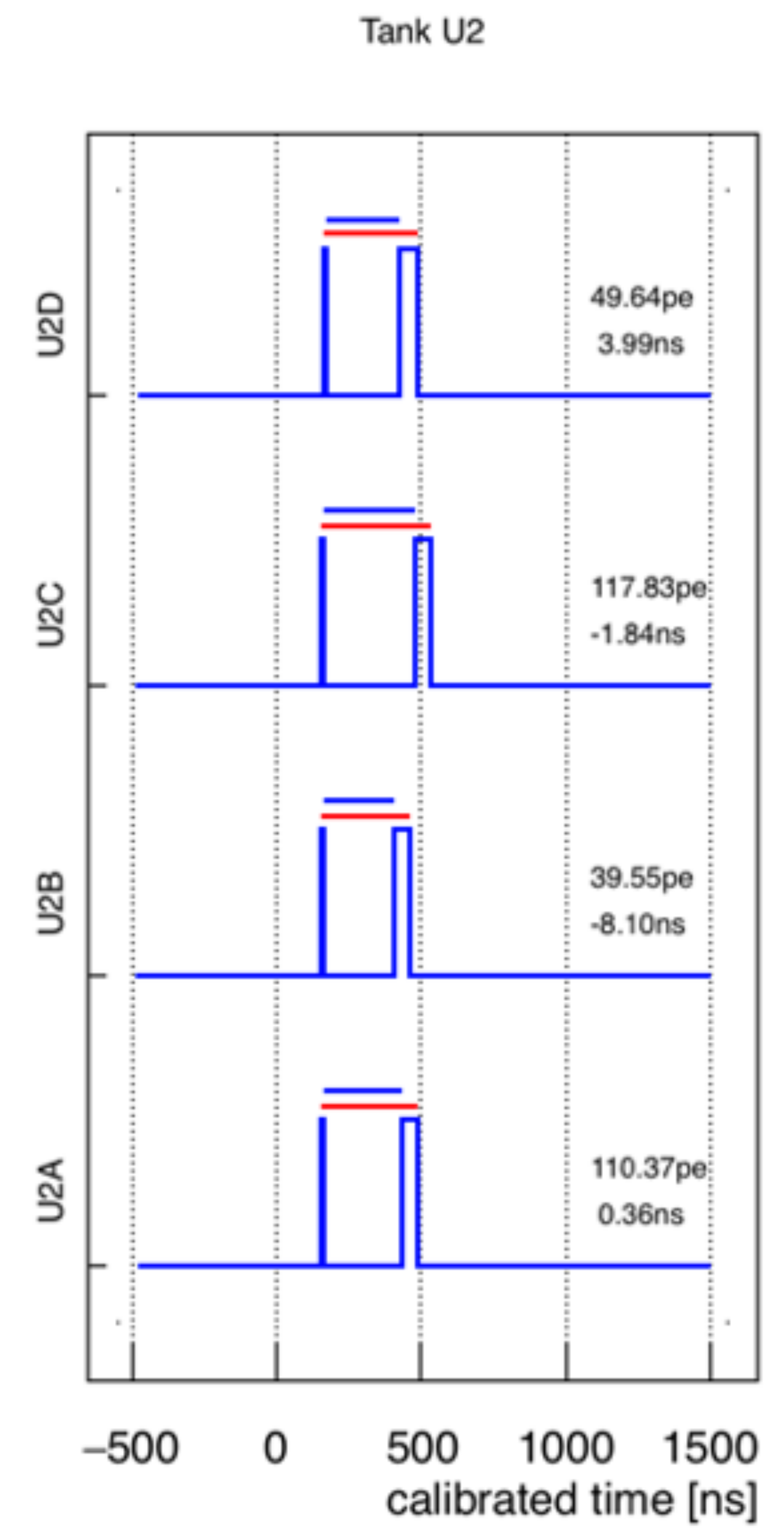

HAWC-250 Event

- Large event, successful fit, probably a cosmic ray

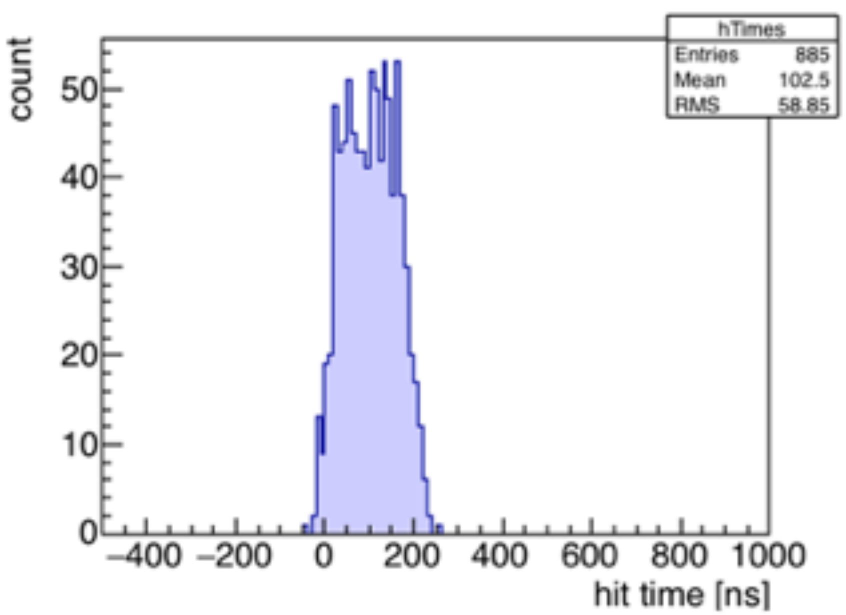

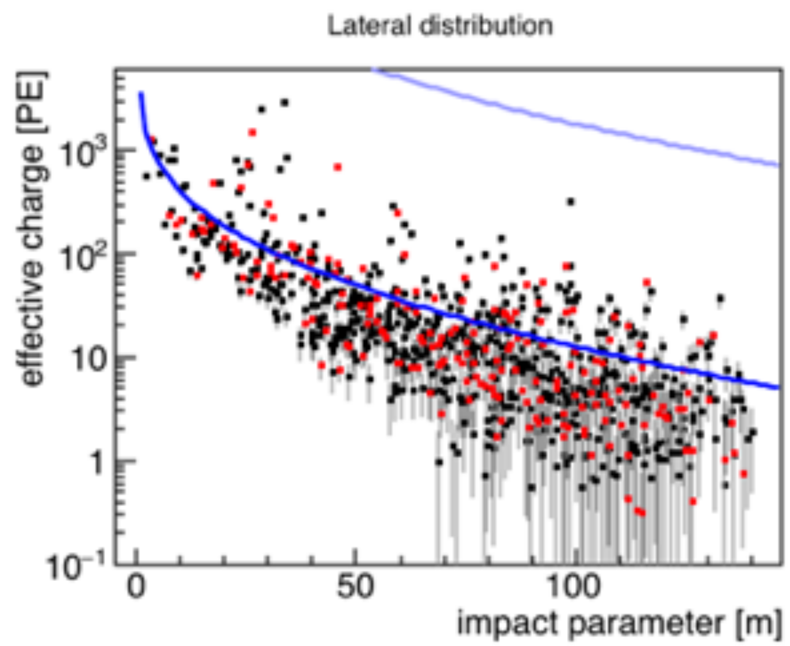

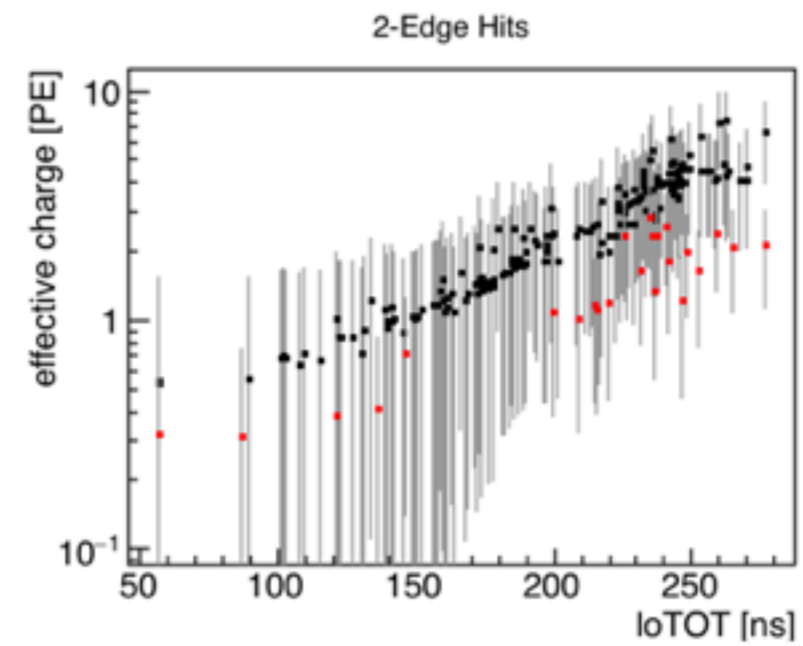

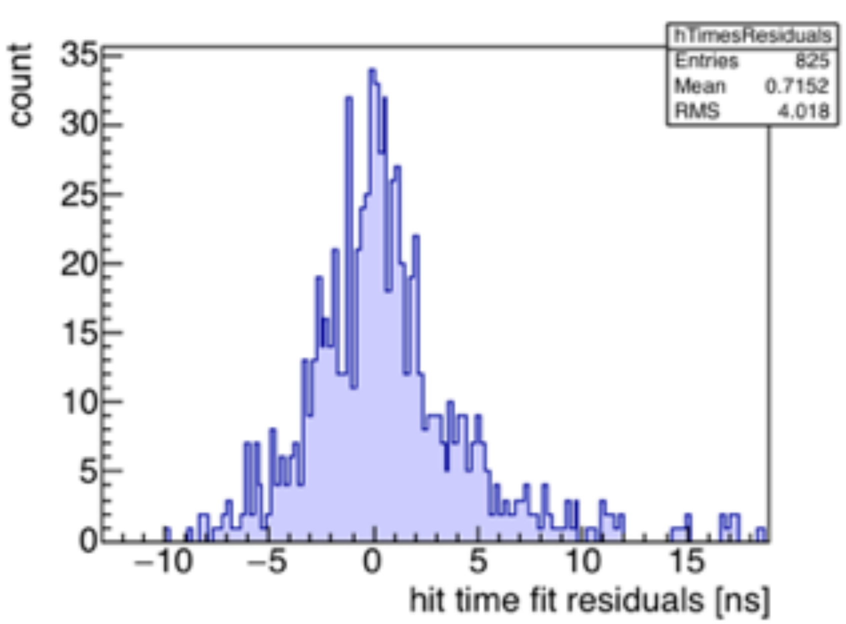

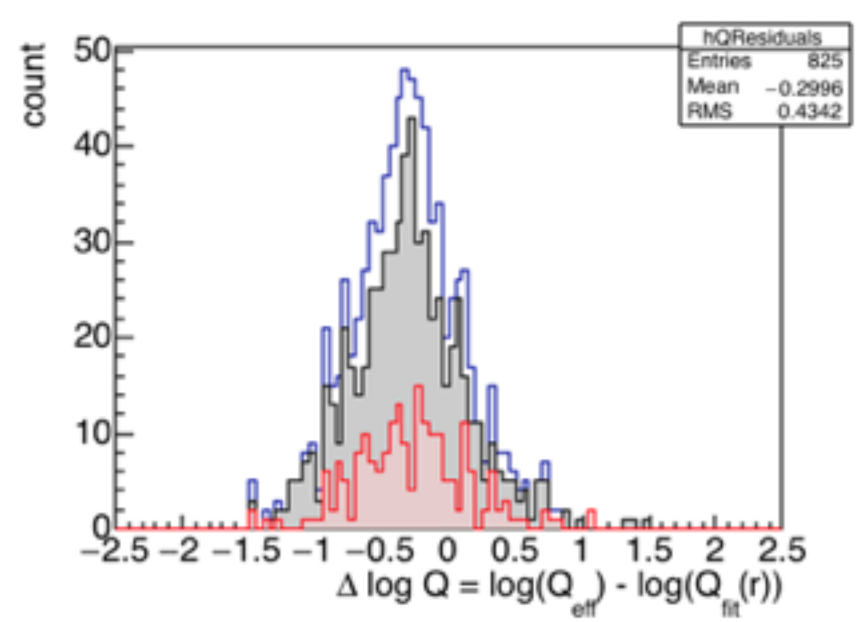

Summary: Run 2105, Time Slice 140025, Event 89
time (GPS): 1101151461 s 195457142 ns
time (UTC): 2014-11-27 19:24:05
Nhit: 825 hits; 976 (tot); 779 (SP10); 808 (SP20)
Channels: 877 (tot); 848 (avail)
Tanks: 247 (tot); 246 (avail); 246 (hit total); 246 (hit)

Core Fit (SUCCESS)
(x, y, s, log A) = (-9.7 m, 219.6 m), 1.23, 6.40
χ^2/ndf (Nhit) = 193544.9 / 873 (825) = 221.7 (234.6)

Angle Fit (SUCCESS)
(ϑ, φ) = (27.7°, -5.1°)
χ^2/ndf = 4735.5 / 822 = 5.8

Compactness
CxPE40 = 682.5
PMT: S12C, XnCh: 143, SPTime: 7.3 ns
compactness: Nhit/CxPE40 = 1.2


SHE'S BEHAVING LIKE A BABY! EVERYTHING IS PERFECT!
YEAH, EXCEPT THE COSMIC RAYS! NO ONE KNOWS WHAT THEY'LL DO...
9

Observations of Cosmic Rays

- We have been observing cosmic rays with very high event rates (20 kHz) since turning on the array
- Angular resolution for cosmic-ray reconstruction ranges from >1° below 1 TeV to <0.5° above 10 TeV
  - Easily sufficient for study of "small-scale" anisotropy of cosmic rays
- Rest of this talk:
  - Observation of the lunar shadow in cosmic rays
  - Observation of 10^{-4} anisotropy in CR intensity

Selected Previous Results

M. Amenomori et al., ApJ **626**:L29, 2005

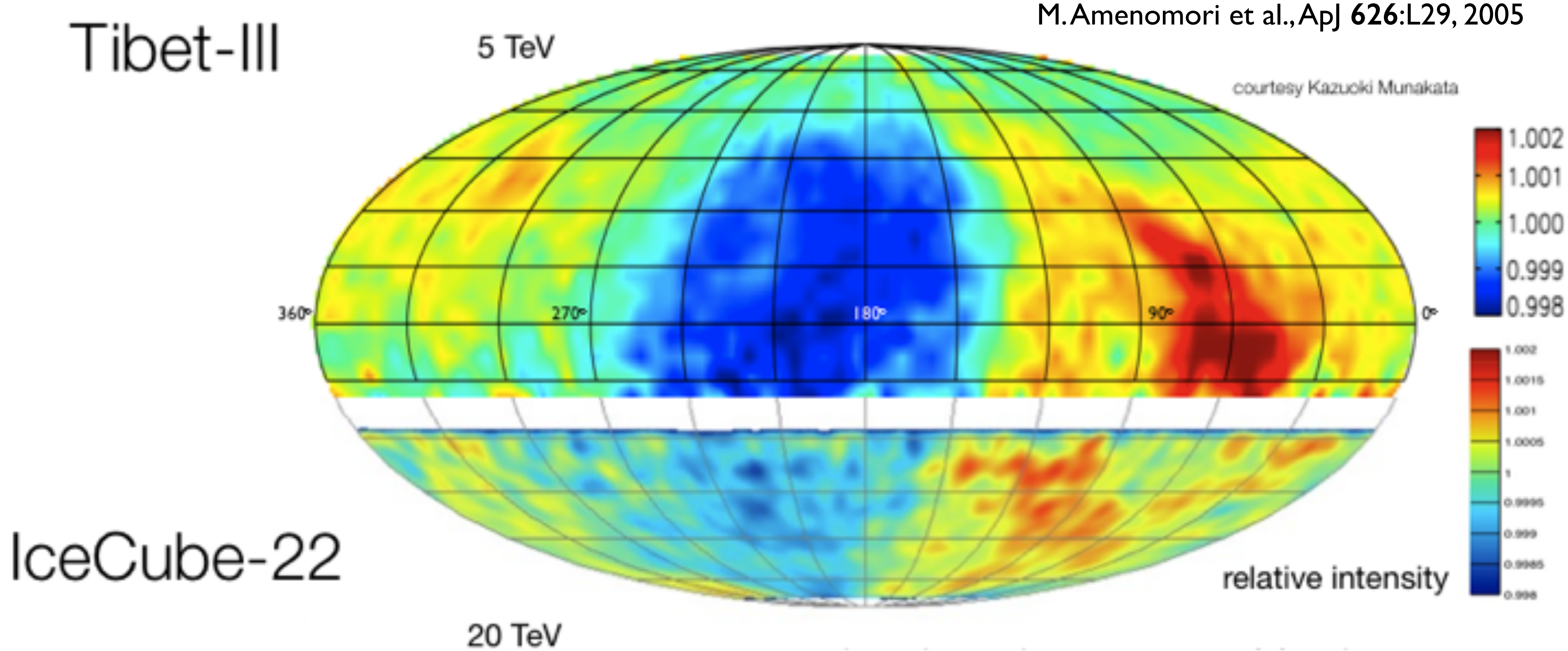

R. Abbasi et al., ApJ **718**:L194, 2010

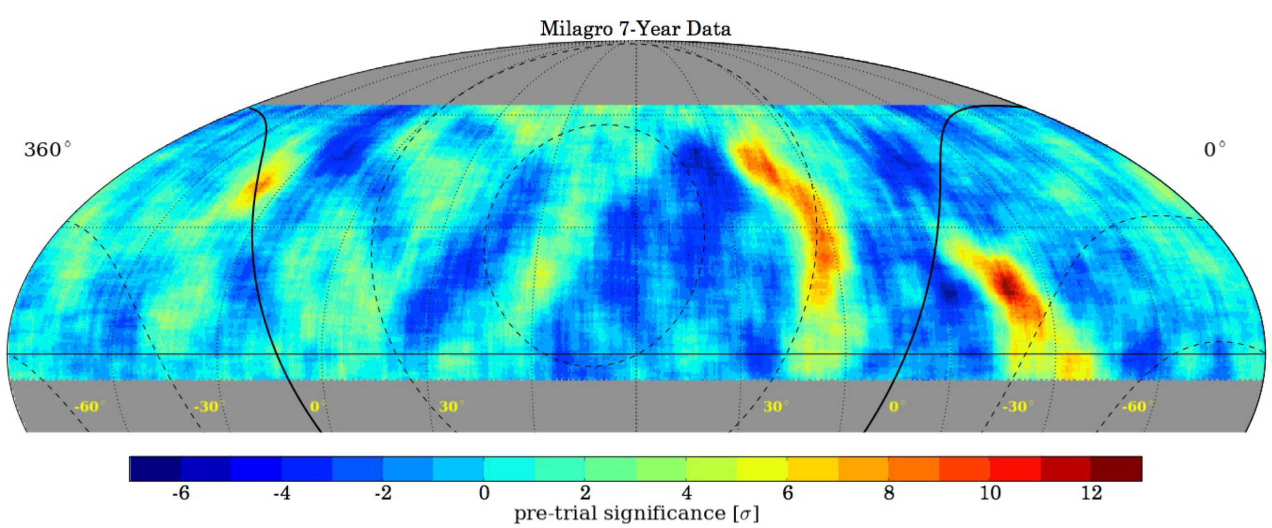

A. Abdo et al., PRL **101**:221101, 2008

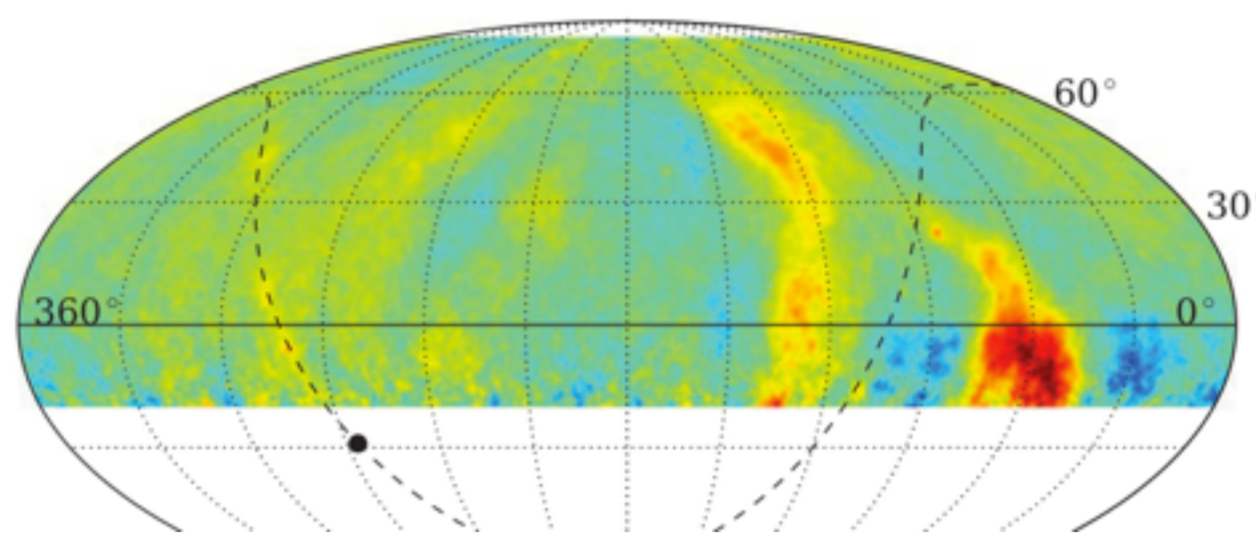

R. Bartoli et al., Phys Rev D**88**:082001, 2013

Detector Configuration

- Reporting results from HAWC-95 and HAWC-111
- 12 Jun 2013 to 8 Jul 2014
- 181 days (4332.1 hr)
- 85.6 billion events
- Event selection:
  - Full runs: contiguous 24 hr periods of observation
  - Successful angle fit
  - $N_{ch} \geq 30$
- 113 days, 49 billion events

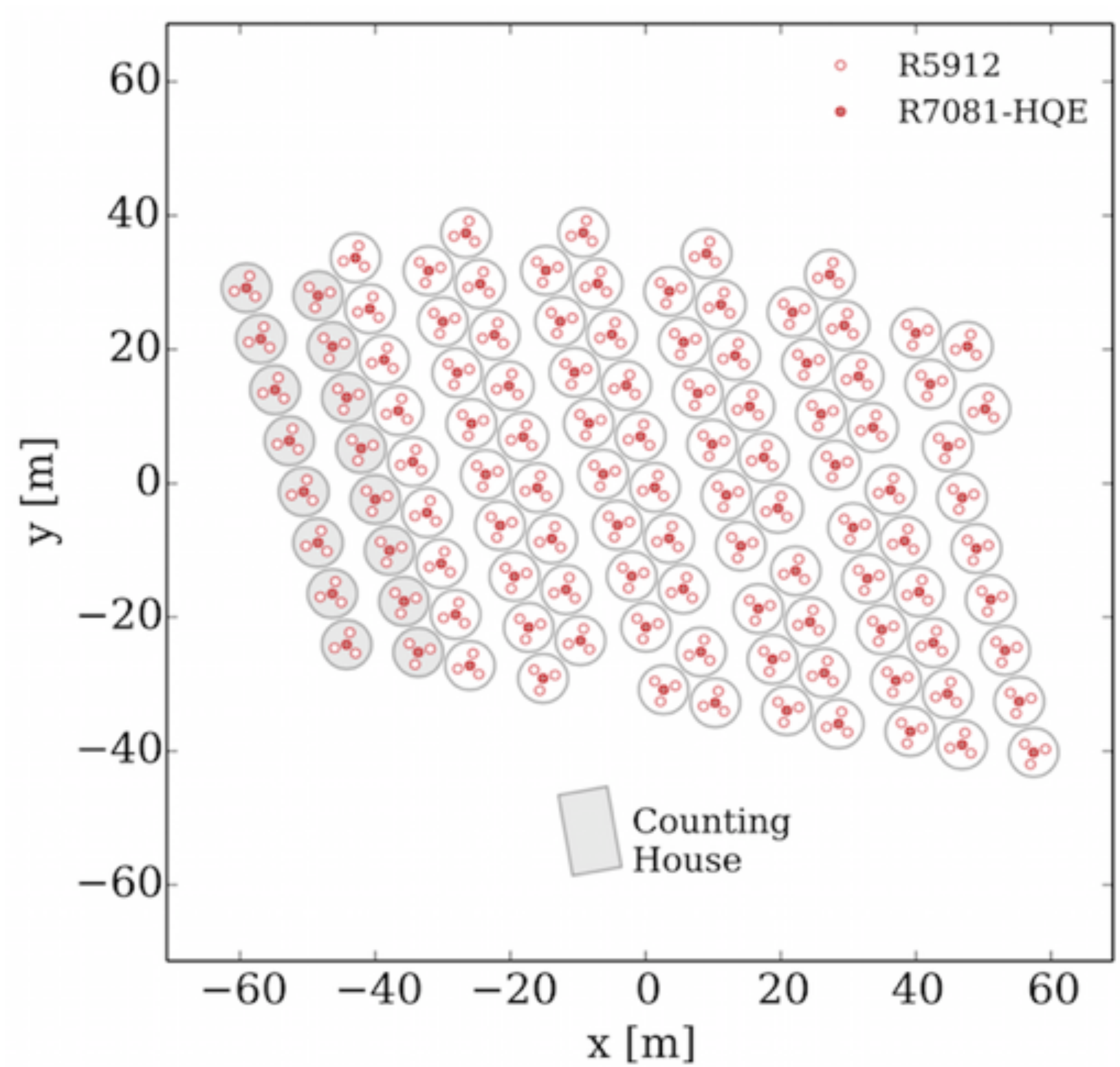

Quantities of Interest

- We report relative intensity (flux integrated above threshold *E*) in a finely-binned map of the sky:

$$\delta I_i(\alpha,\delta) = \frac{\Delta N_i}{\langle N \rangle_i} = \frac{N_i(\alpha,\delta) - \langle N_i(\alpha,\delta)\rangle}{\langle N_i(\alpha,\delta)\rangle}$$

$$\delta I(\alpha_i,\delta_i) = \sum_{\ell=0}^{\infty}\sum_{m=-\ell}^{\ell} a_{\ell m} Y_{\ell m}(\pi-\delta_i,\alpha_i)$$

- Expected counts affected by detector and atmospheric fluctuations. Use data to estimate expected counts
- Sky maps may be rebinned/smoothed to enhance the appearance of significant features
- Statistical significance reported in terms of Gaussian σ

Background Estimation

- Effect of atmosphere, detector drift on event rate:

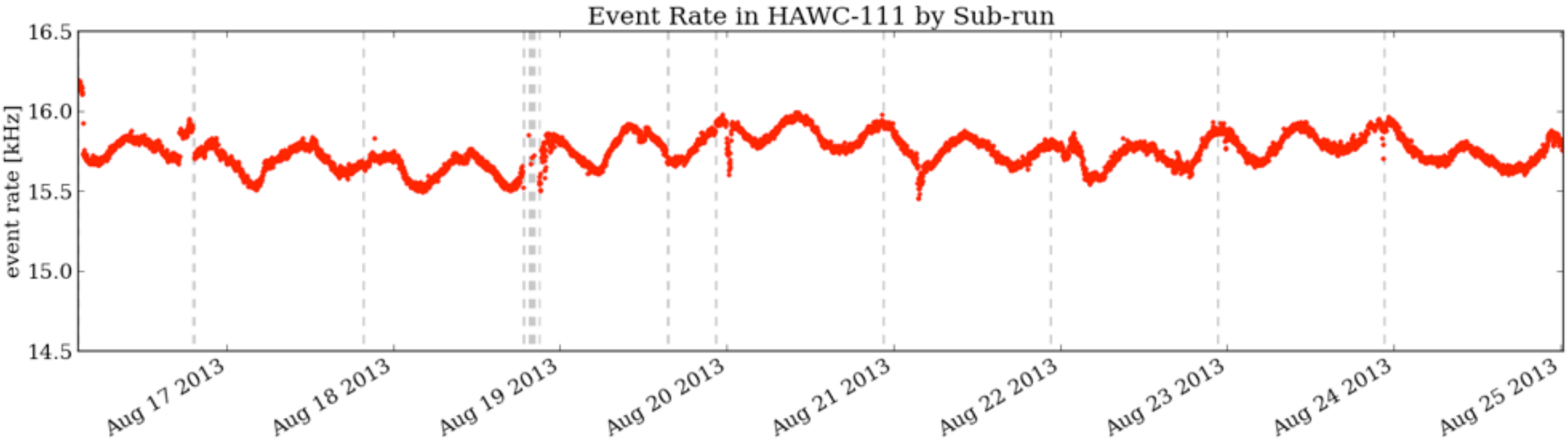

- Use data from interval *dt* to get the expected counts

$$\langle N(\alpha,\delta)\rangle = \int dt \int d\Omega\ \underbrace{A(ha,\delta)}_{\text{Detector acceptance}} \cdot \overbrace{R(t)}^{\text{Event rate}} \cdot \underbrace{\epsilon(ha,\alpha,t)}_{\text{Selection function: 1 if } ha,\,\alpha,\,t \text{ in same bin}}$$

Energy of the Data Set

- Simulated data with CORSIKA + GEANT4 model
- Median energy of sample: 2 TeV
- Median angular resolution: 1.2°
- Note: data include gamma ray showers, which have better angular resolution than cosmic rays

A. Abeysekara et al., ApJ **796**:108, 2014

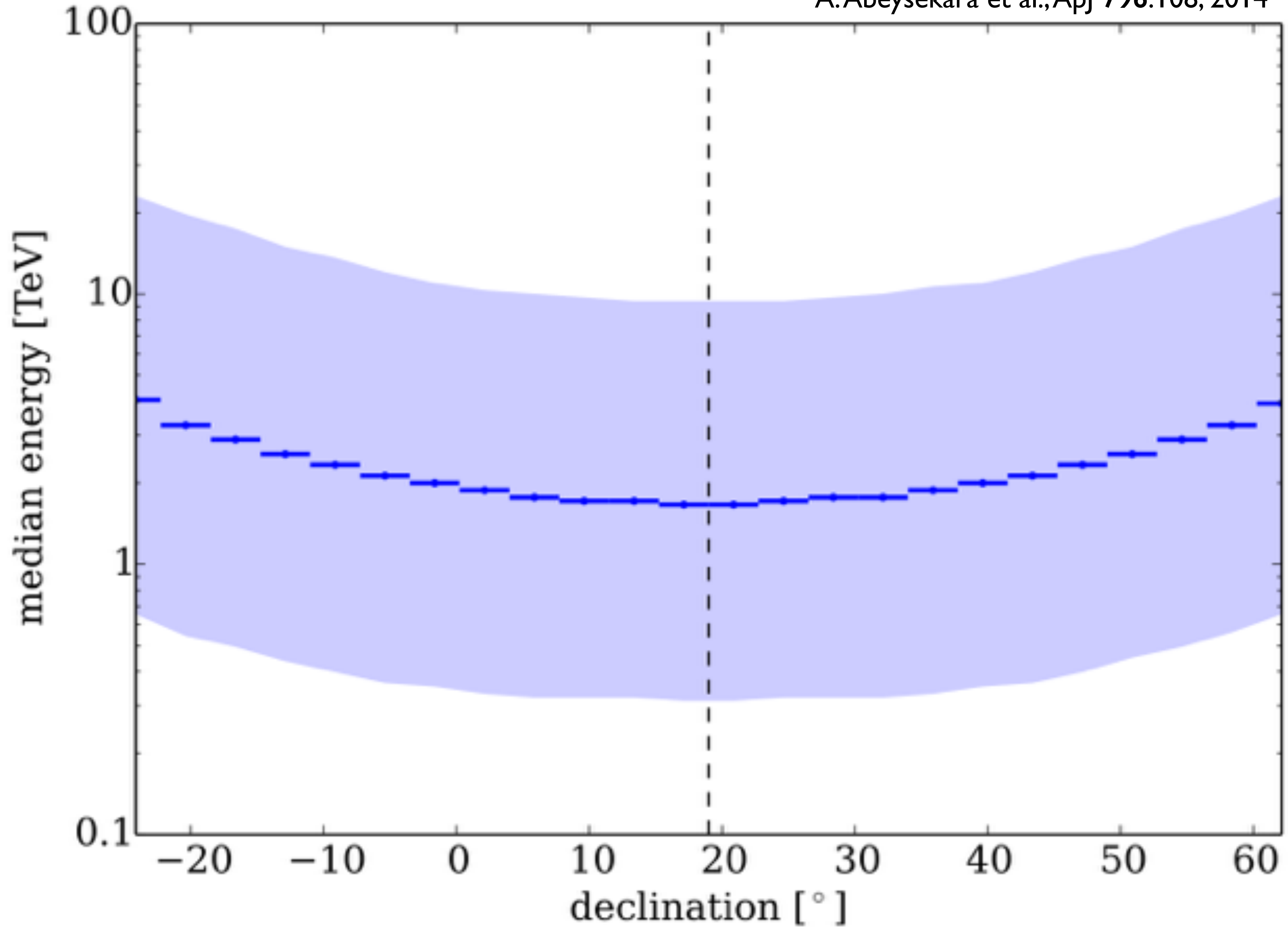

Geomagnetic Effects

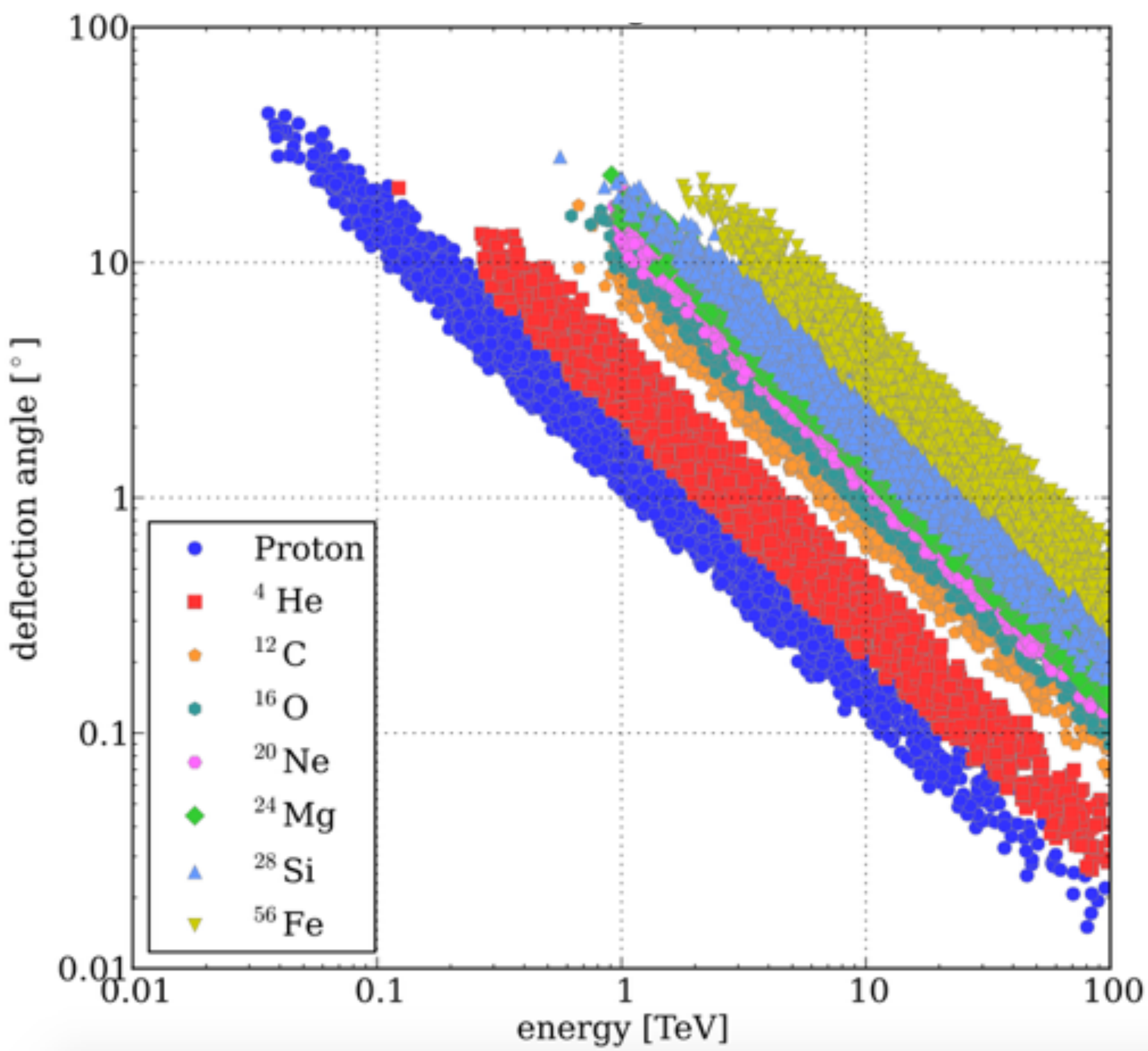

- At and below ~2 TeV, the deflection of cosmic rays in the geomagnetic field is larger than the angular resolution of the detector
- Left: simulated deflection per species at location of HAWC using IGRF11 field
- Best fit for cosmic-ray deflection at HAWC site:

$$\delta\theta \simeq 1.6^\circ \cdot Z \left(\frac{E}{\text{TeV}}\right)^{-1}$$

Detection of Moon Shadow

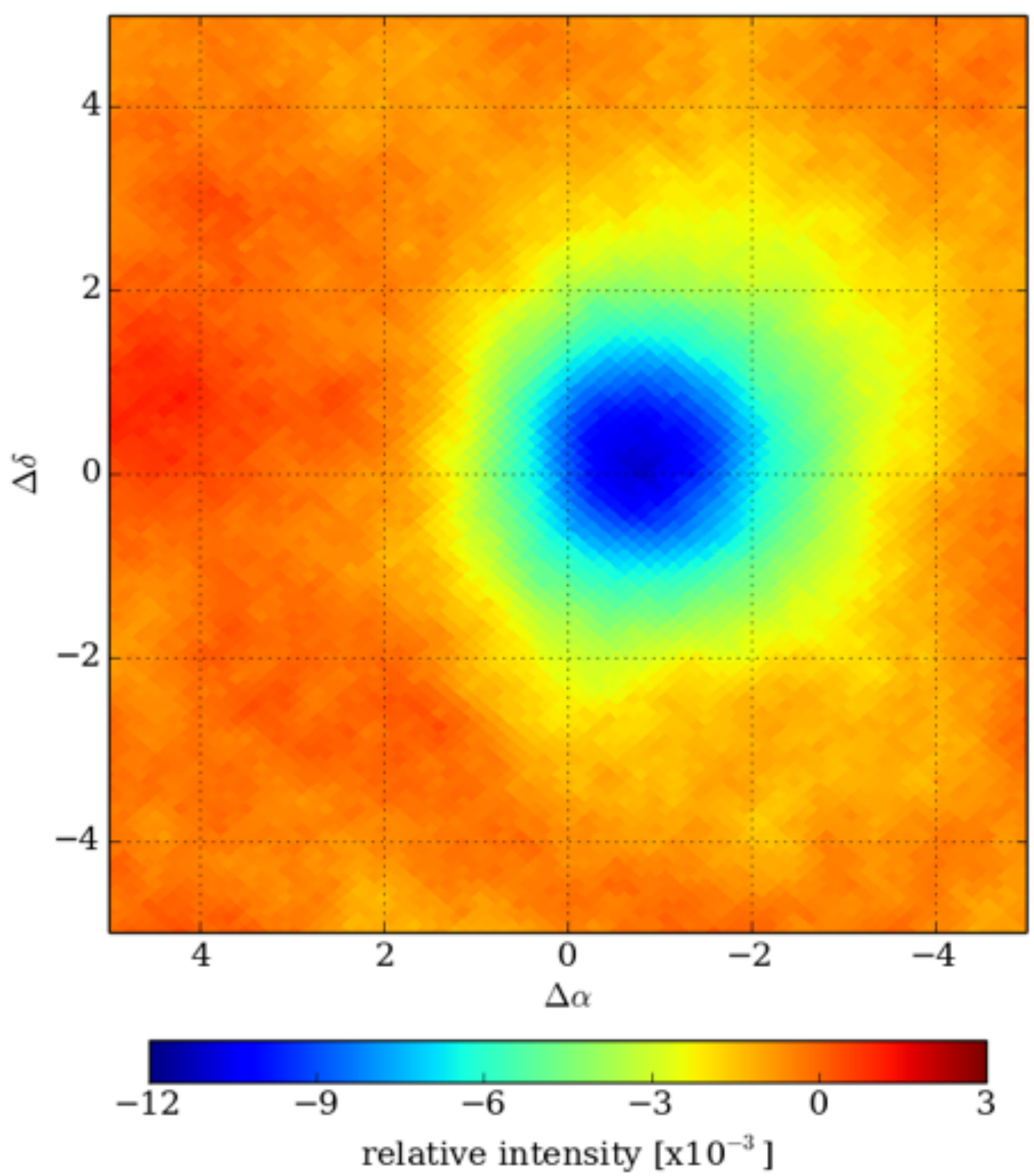

- 181 transits, -32.5σ
- Significance:
  - 2.4σ /√transit
- deflection: -0.91°±0.04°, (recall: E_{median} = 2 TeV)
- Relative intensity:
  - $(-11.3 \pm 0.4) \times 10^{-3}$
- Position verifies pointing

Detection of Moon Shadow

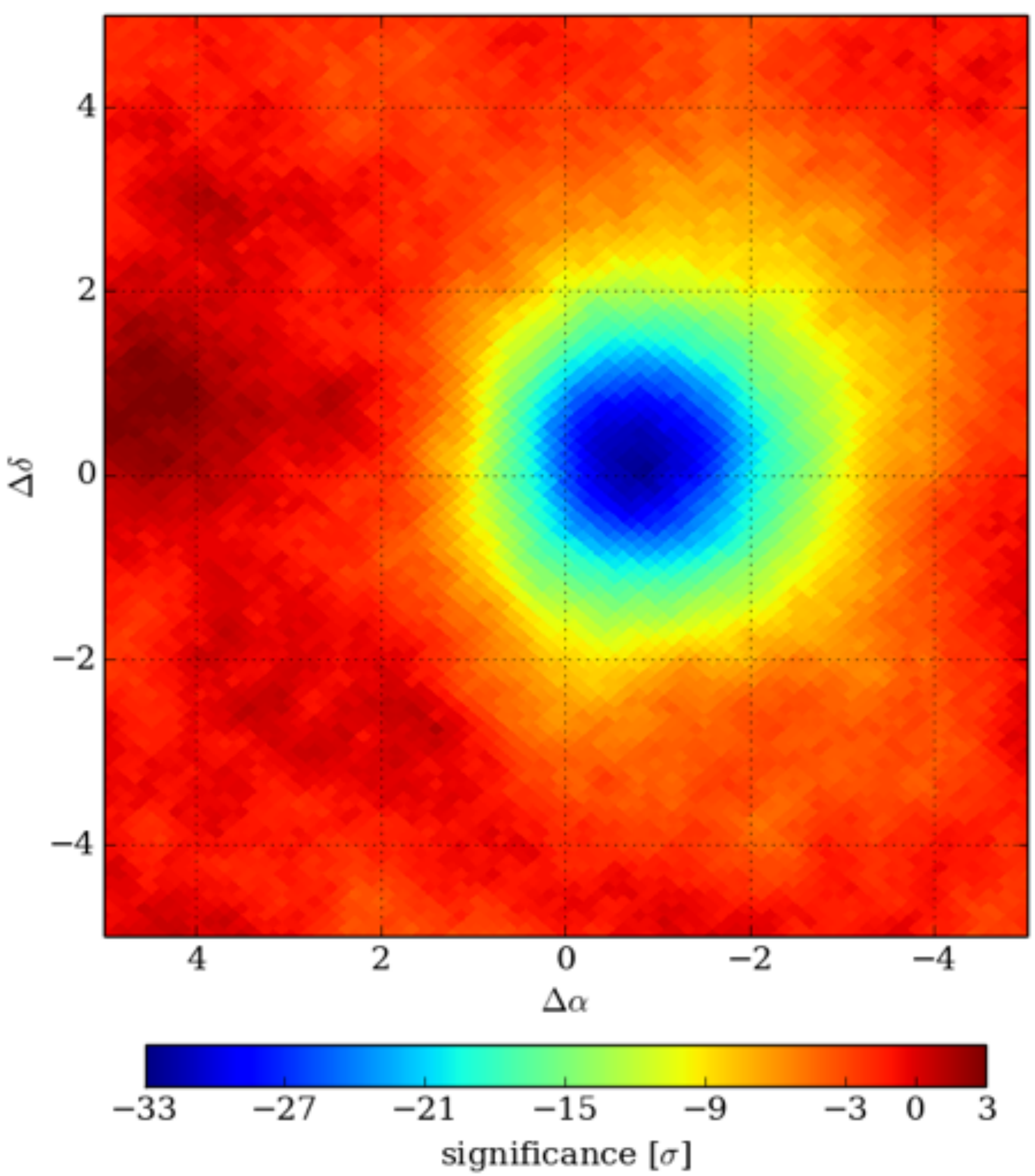

- 181 transits, -32.5σ
- Significance:
  - 2.4σ /√transit
- deflection: -0.91°±0.04°, (recall: E_{median} = 2 TeV)
- Relative intensity:
  - $(-11.3 \pm 0.4) \times 10^{-3}$
- Position verifies pointing

Relative Intensity Map

- Binned skymap, *dt*=24 hr, 10° smoothing filter applied:

A. Abeysekara et al., ApJ **796**:108, 2014

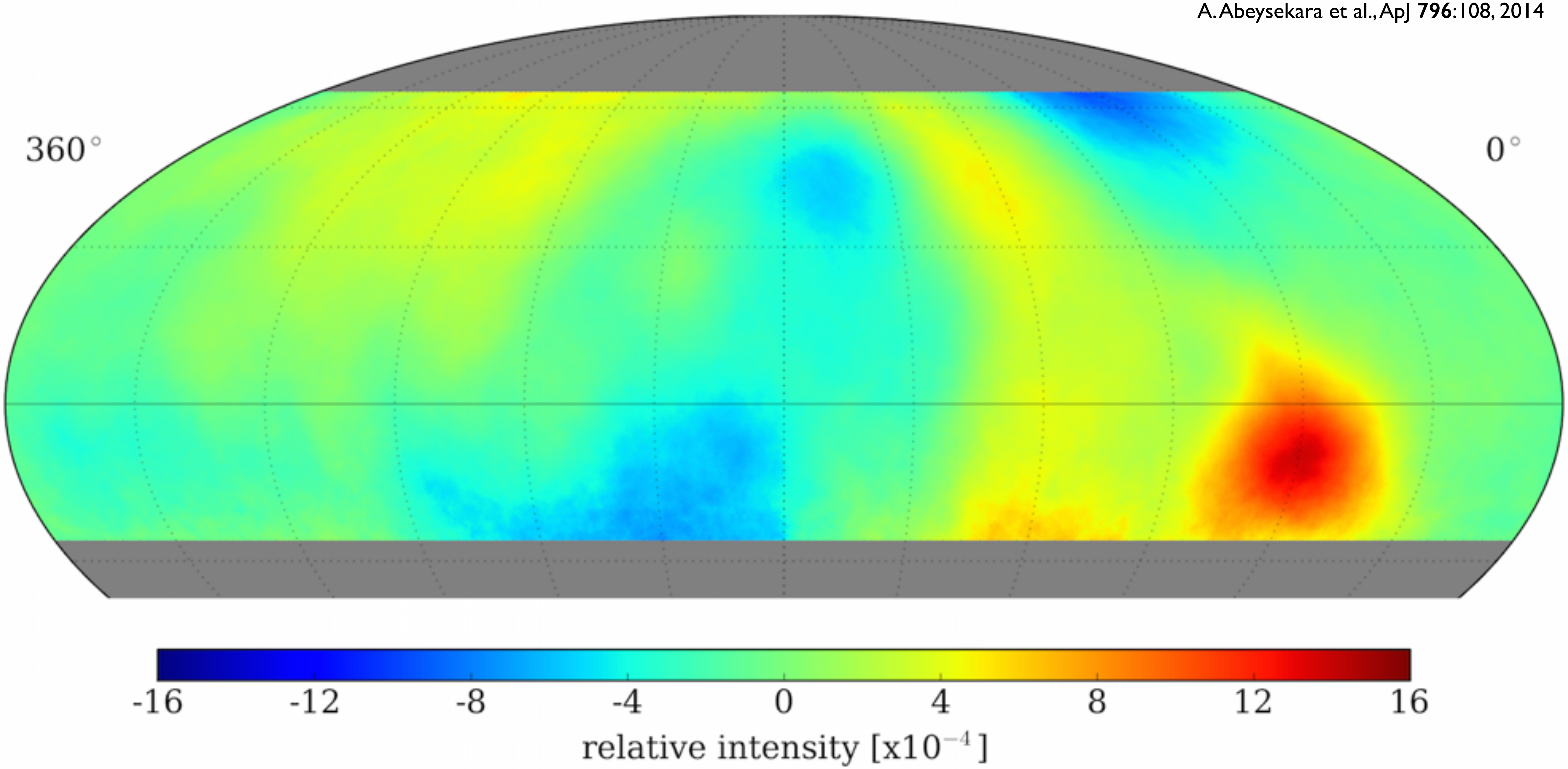

Large-Scale Features?

- Other measurements of anisotropy (e.g., IceCube) indicate a dipole-like structure at these energies. Why is it not obvious in this map?
- Uncorrected systematic effects:
  - Correction needed for running at mid-latitude (full sky not visible instantaneously)
  - Correction needed for partial year coverage and contamination due to "solar dipole" effect
- Our choice: wait for a complete year of data. For now, move on, look for additional structure in the data

Angular Power Spectrum

- Power spectrum indicates presence of structure at small scales. *Not* a partial sky effect, which we correct for.

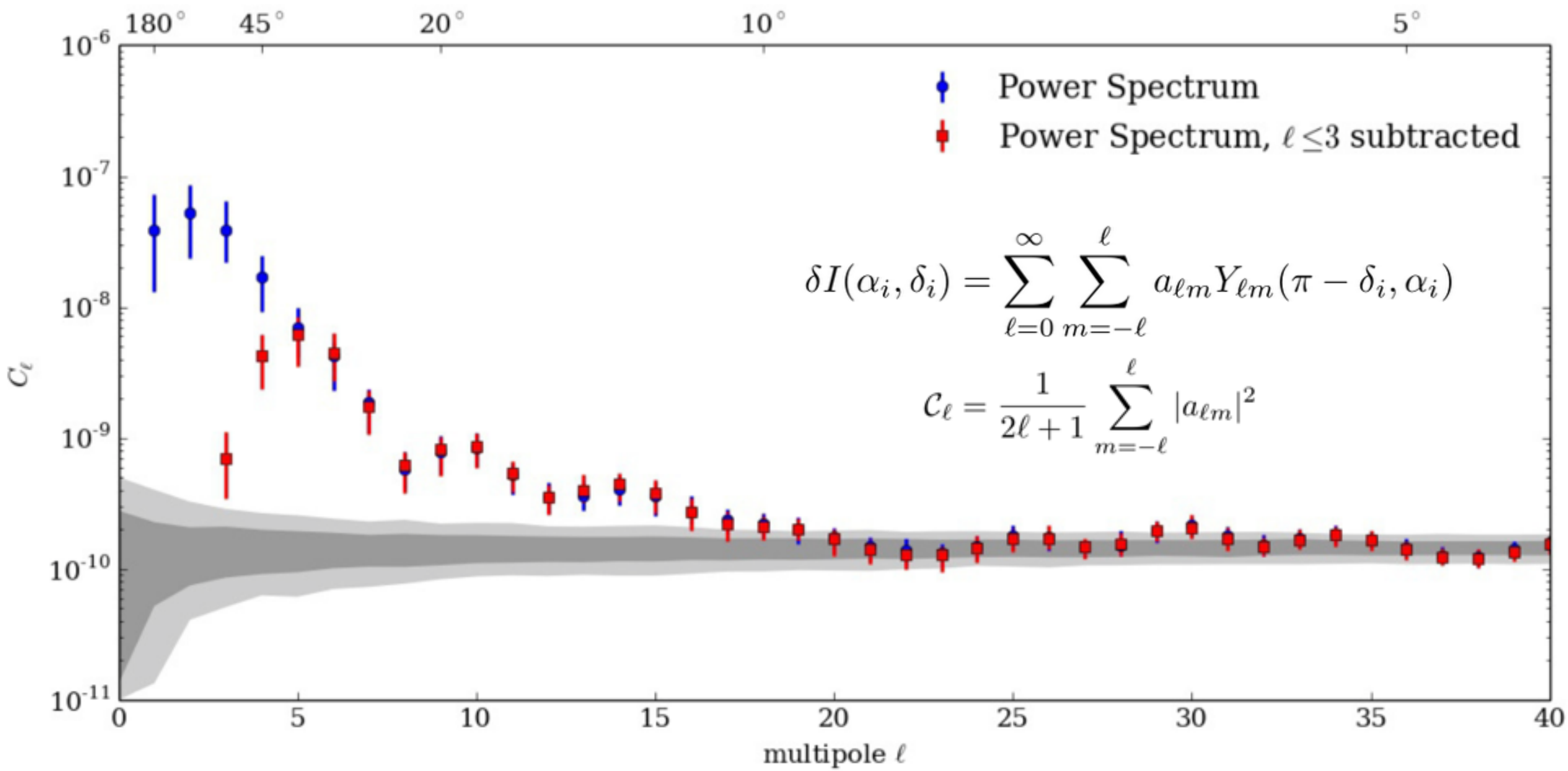

Small-Scale Anisotropy

- Sky map after subtraction of largest features:

A. Abeysekara et al., ApJ **796**:108, 2014

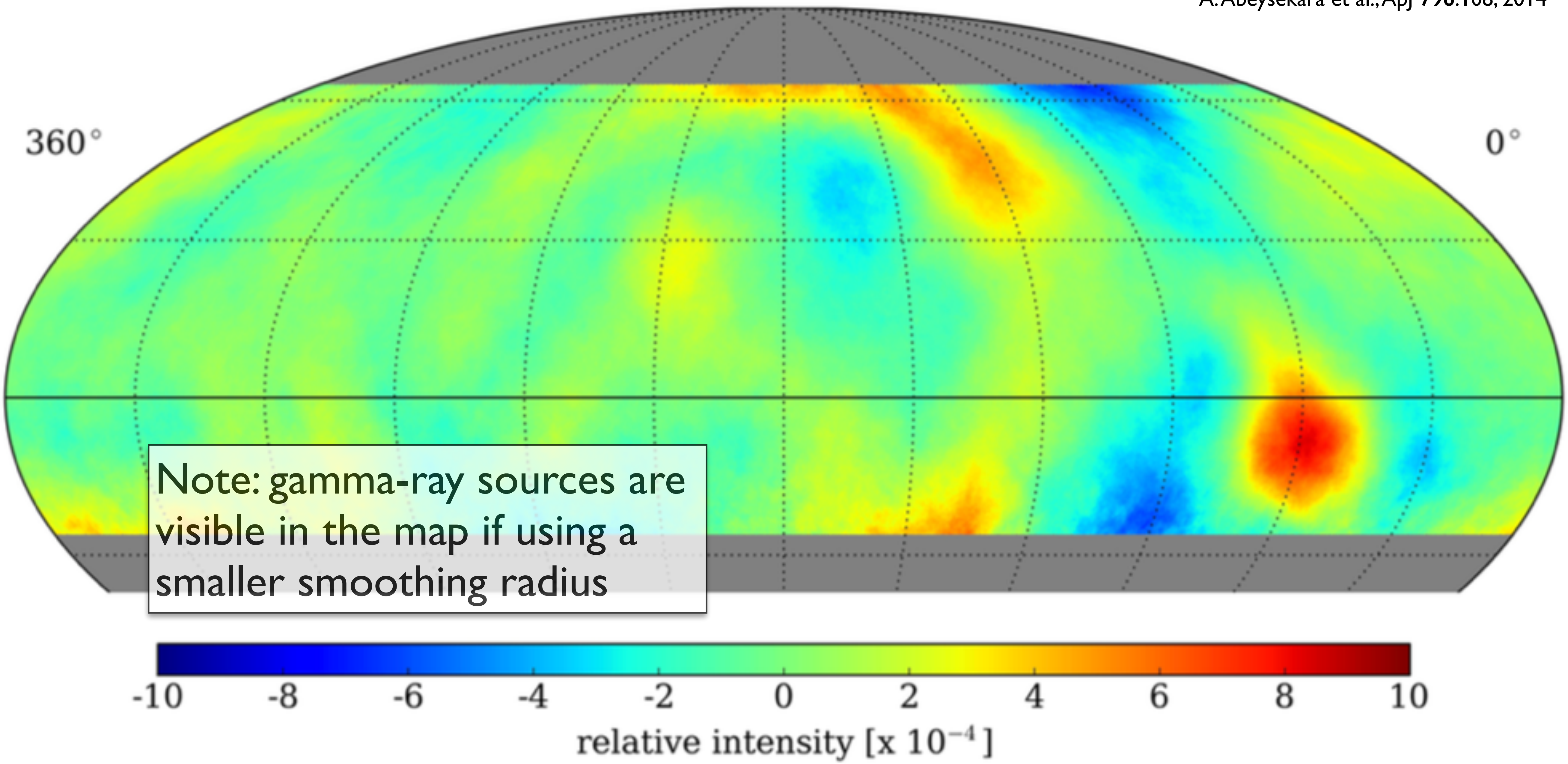

Small-Scale Anisotropy

- Sky map after subtraction of largest features:

A. Abeysekara et al., ApJ **796**:108, 2014

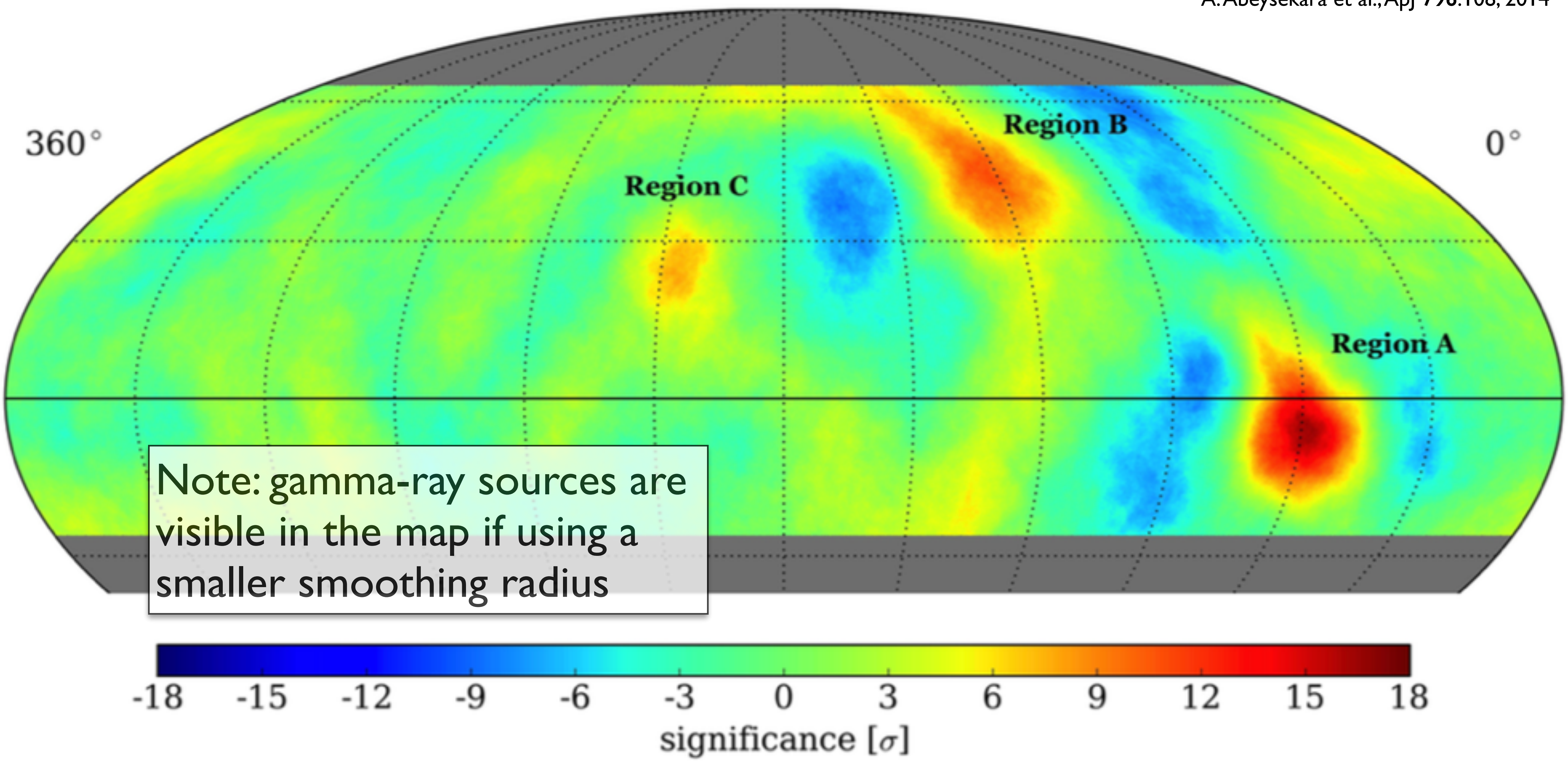

Note: gamma-ray sources are visible in the map if using a smaller smoothing radius

Systematic Check

- Binned skymap, *dt*=4 hr, 10° smoothing filter applied:

A. Abeysekara et al., ApJ **796**:108, 2014

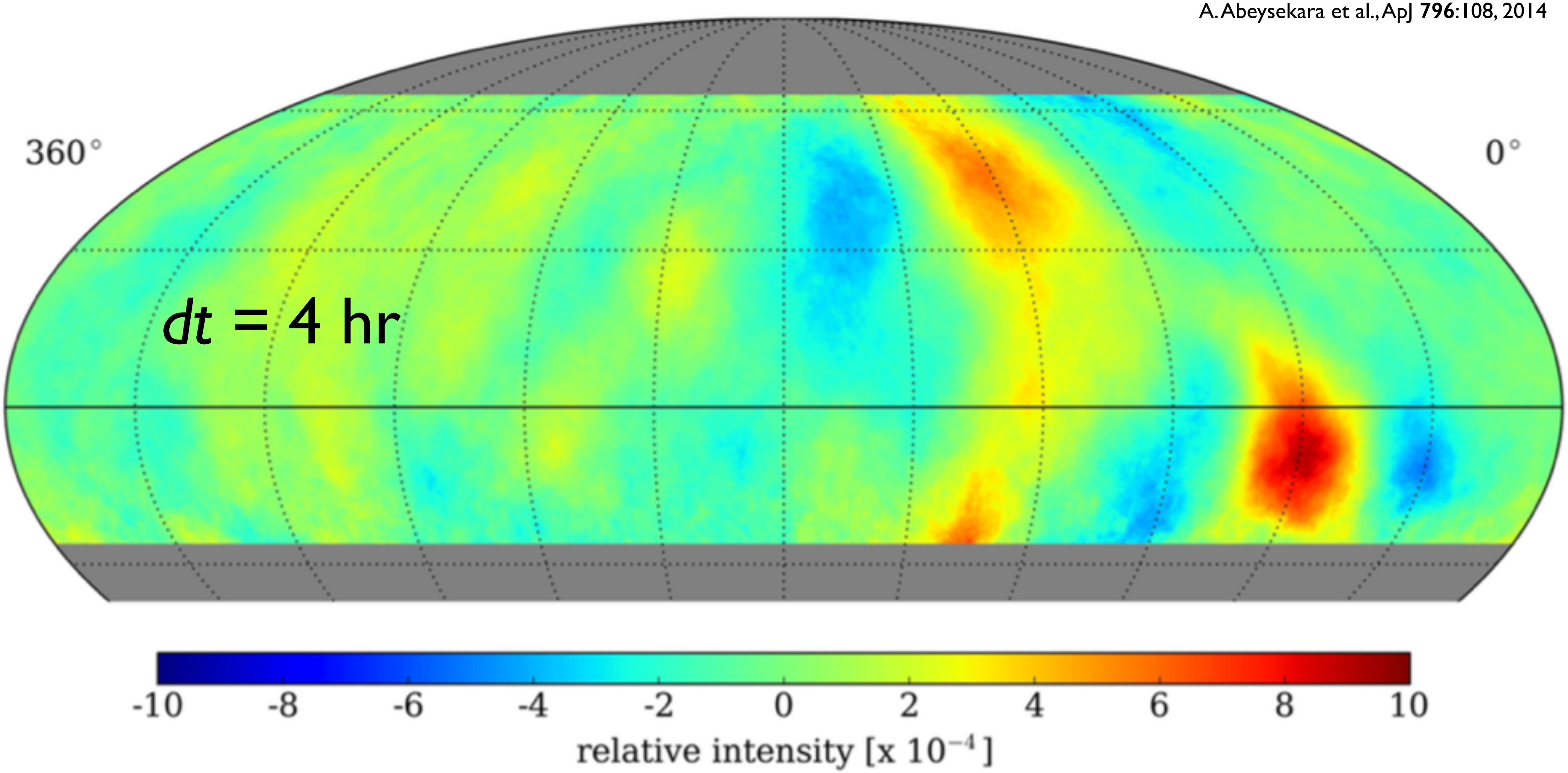

Systematic Check

- Binned skymap, *dt*=4 hr, 10° smoothing filter applied:

A. Abeysekara et al., ApJ **796**:108, 2014

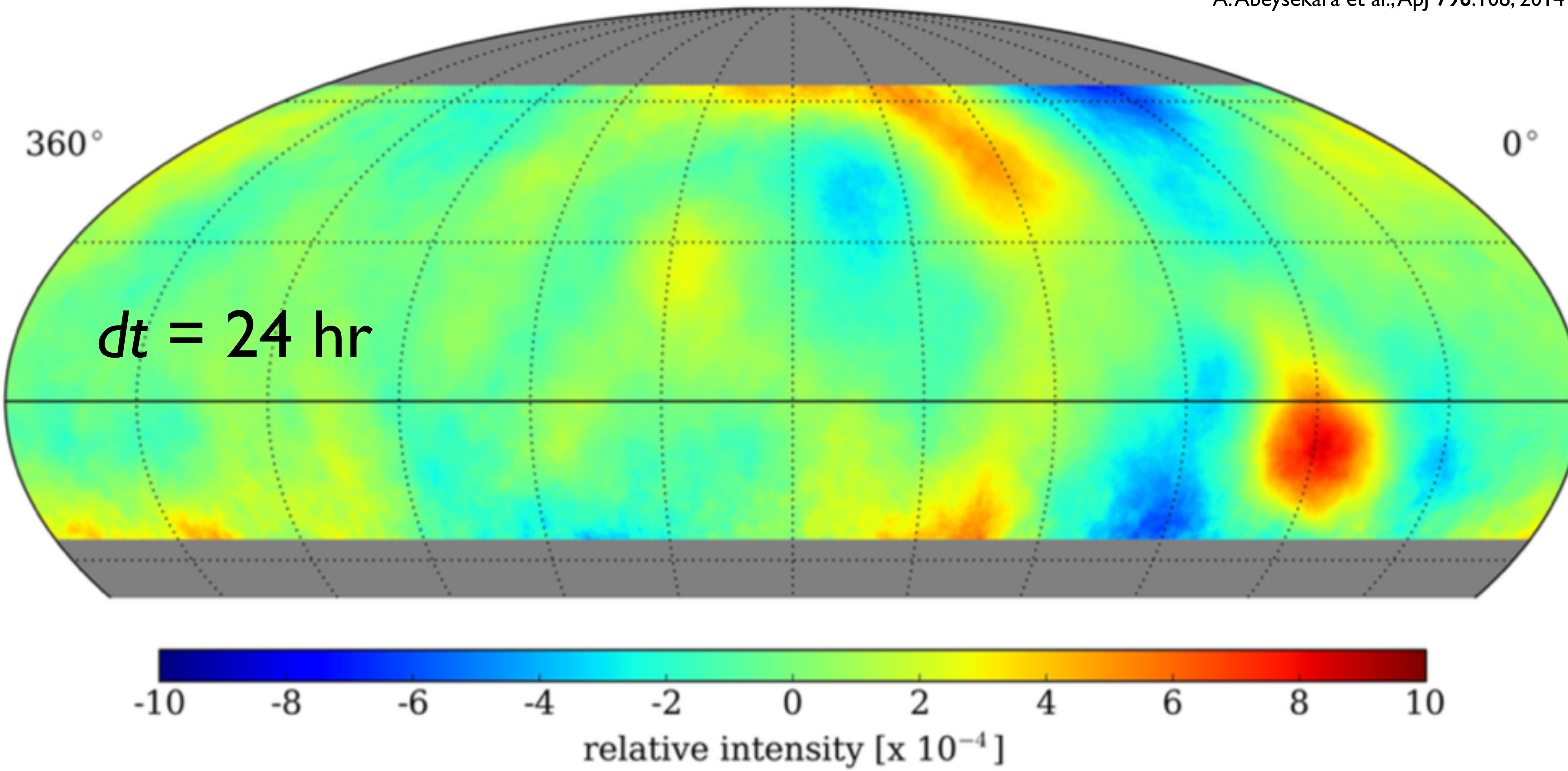

Hotspots

A. Abeysekara et al., ApJ **796**:108, 2014

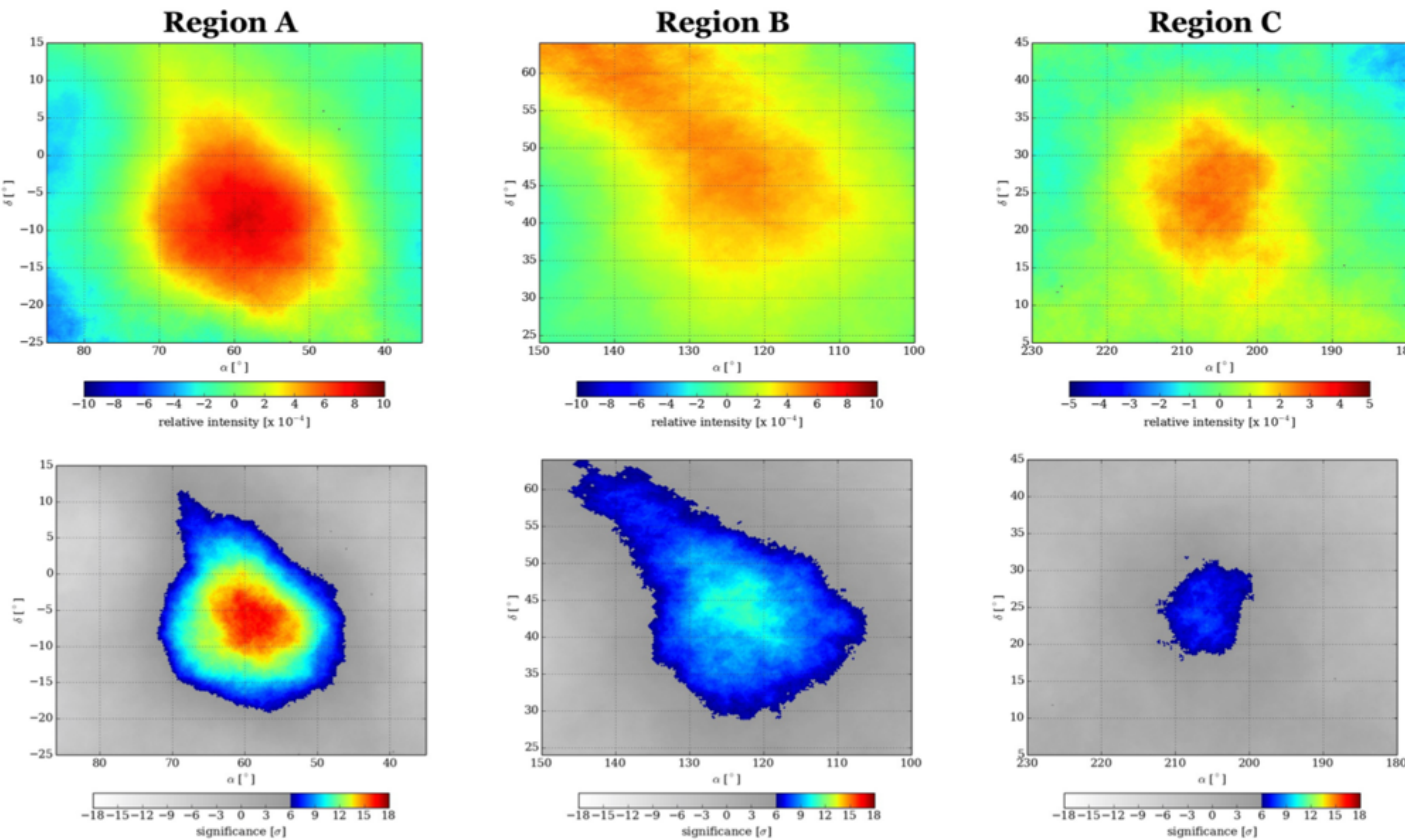

Energy Dependence

- Milagro: power law with cutoff: $f(E) = E^{-\gamma} \exp(-E/E_c)$

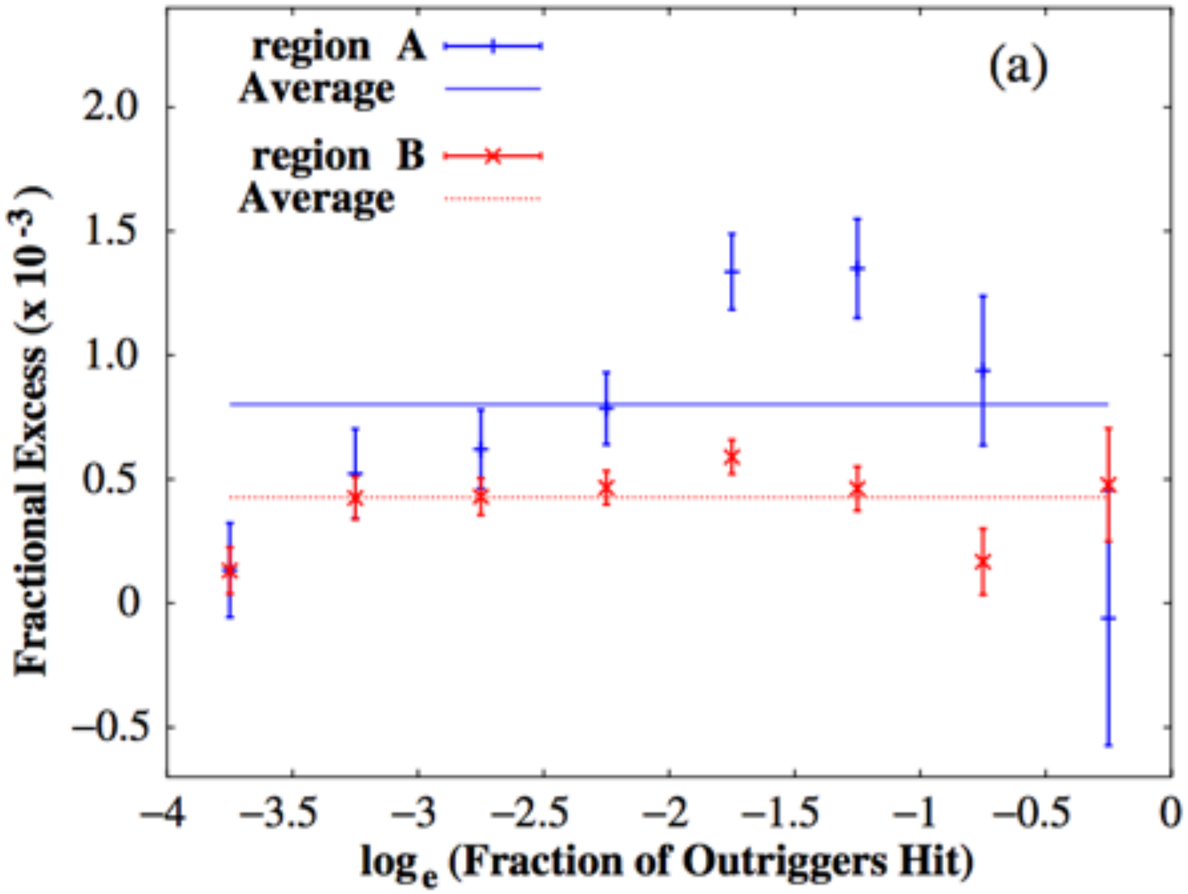

A. Abdo et al., PRL **101**:221101, 2008

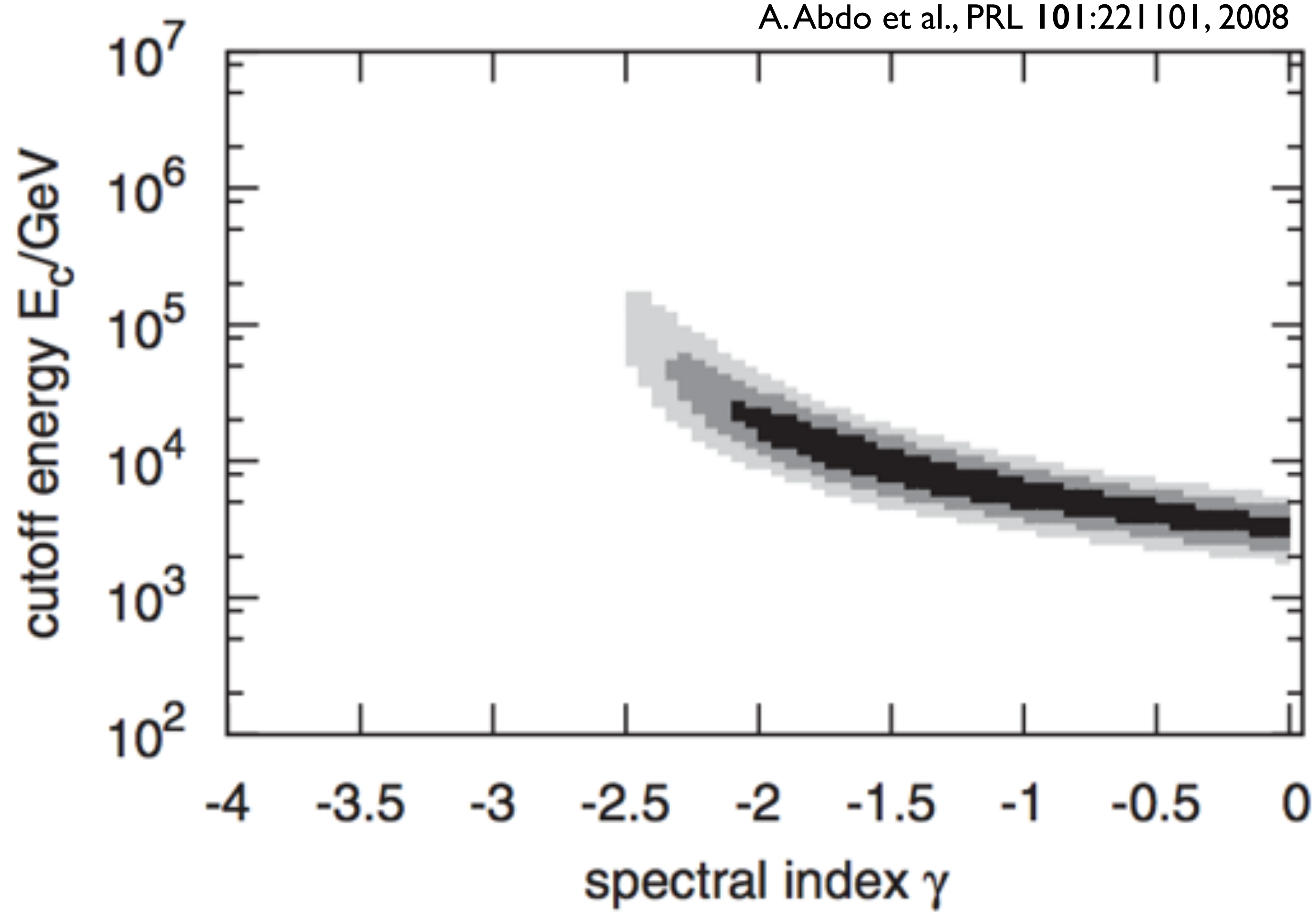

- Hadron-like composition, spectrum harder than $E^{-2.7}$, cutoff E_C = 10.0-6.8+15.1 TeV (stat)

Energy Dependence

- Energy proxy: binning of median energy based on 2D slices in simulated N_{ch} and cos ϑ, similar to IceCube analysis

A. Abeysekara et al., ApJ **796**:108, 2014

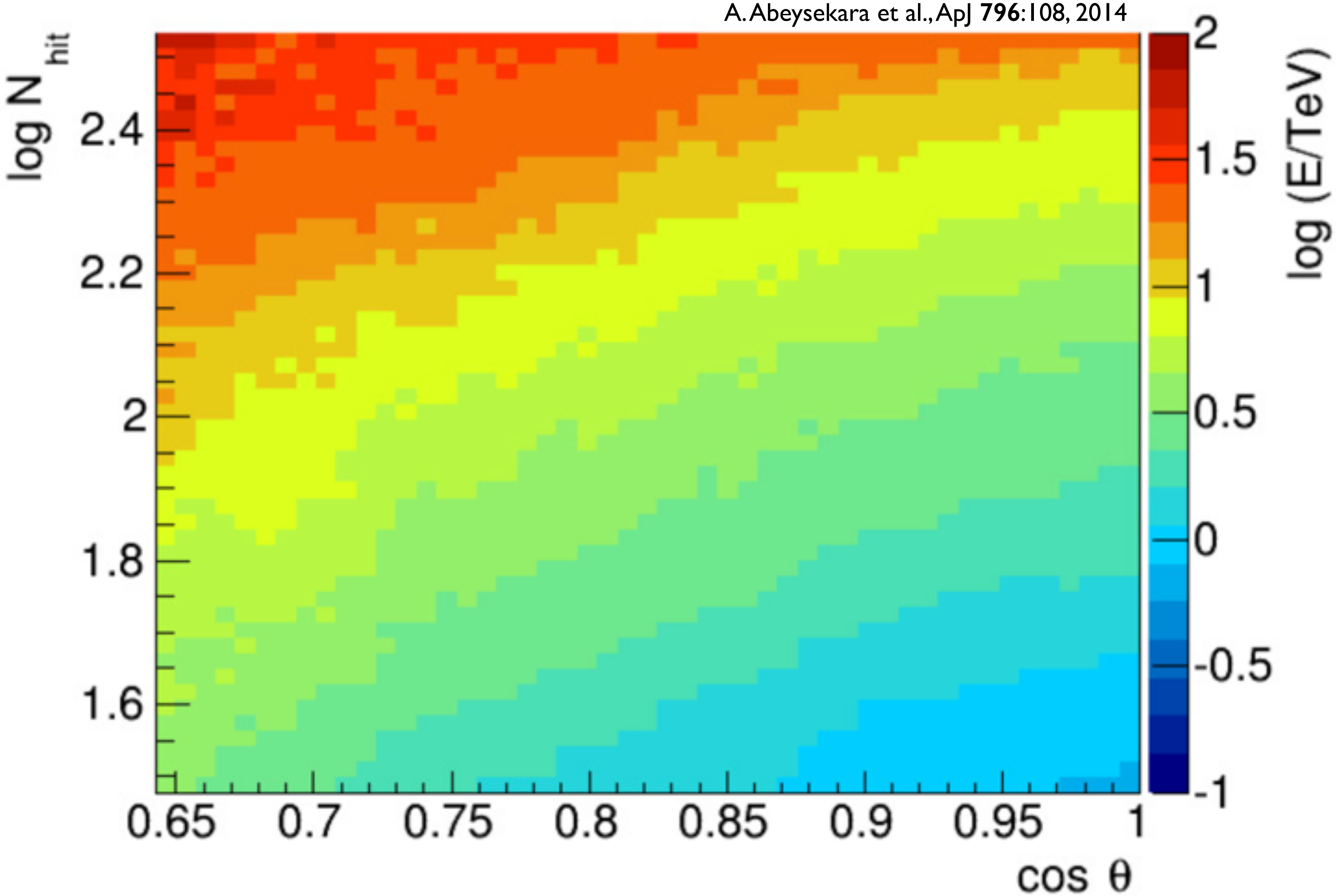

Relative Intensity of Region A

- Relative intensity in 10° circle around region A in 7 bins
- "Hardening" of spectrum in Region A, comparing to off-source regions: 3.8σ effect

A. Abeysekara et al., ApJ **796**:108, 2014

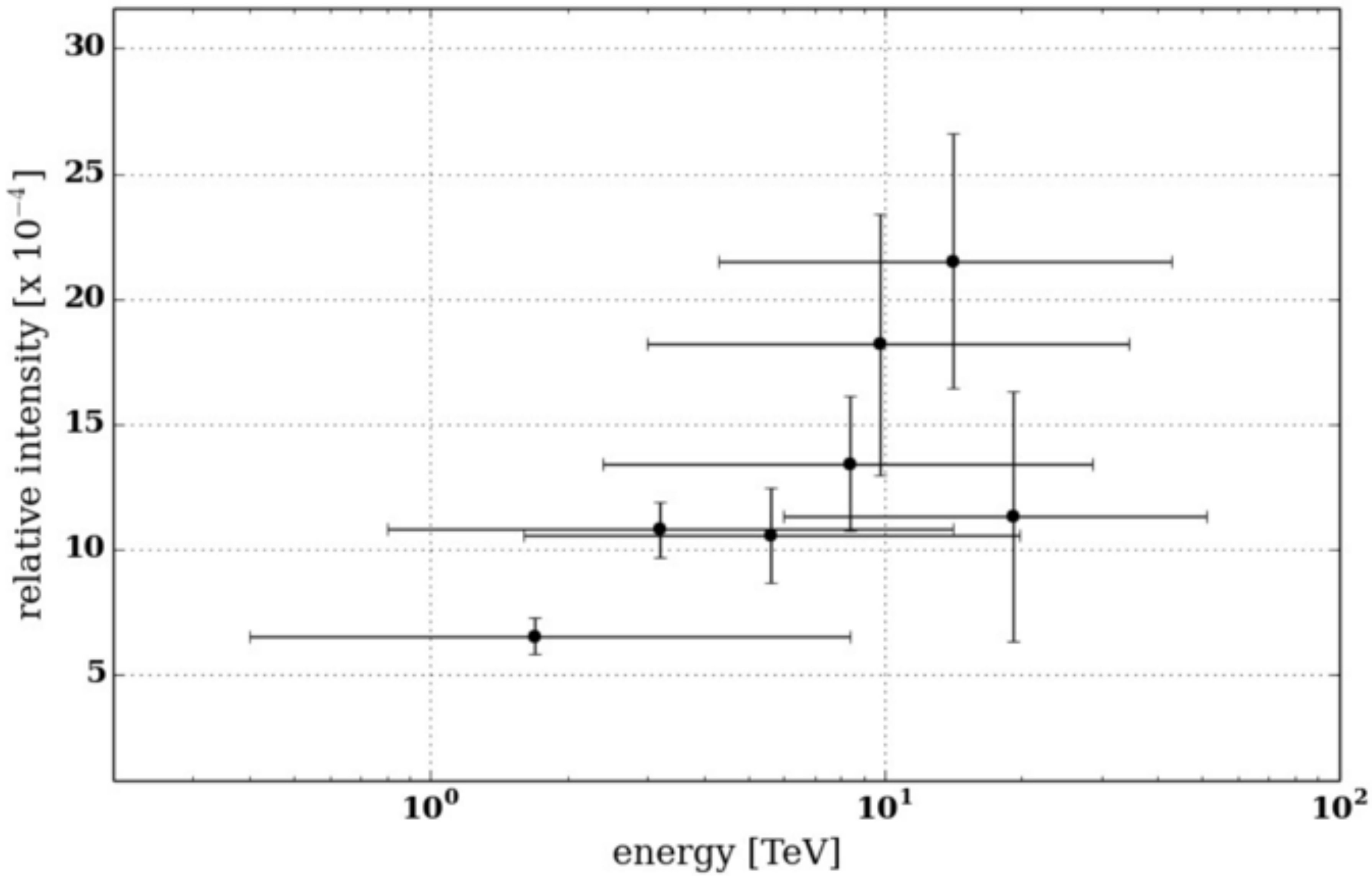

E_{center} = 1.7, 3.2, 5.6, 8.4, 9.8, 14.1, 19.2 TeV

Region A vs Energy Band

- Square = centroid of Region A reported by Milagro, PRL 2008
- Combined δ*I* in bins 4-7 agrees with Milagro amplitude at centroid
- ARGO: δ*I* increases with energy in the upper part of Region A (see Bartoli et al., PRD **88**:2013)

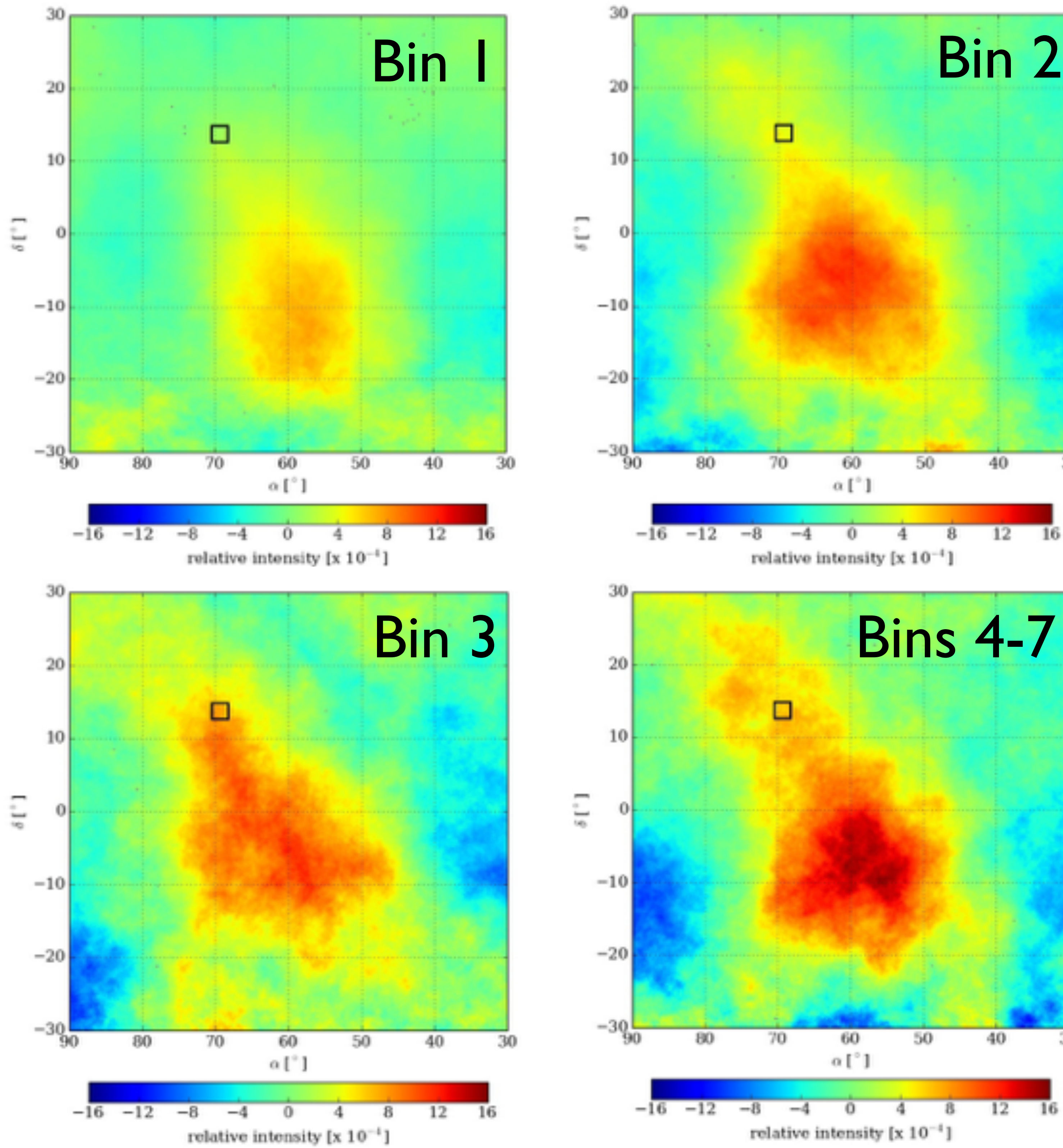

Comparing Previous Results

- Comparison to ARGO-YBJ (different smoothing)

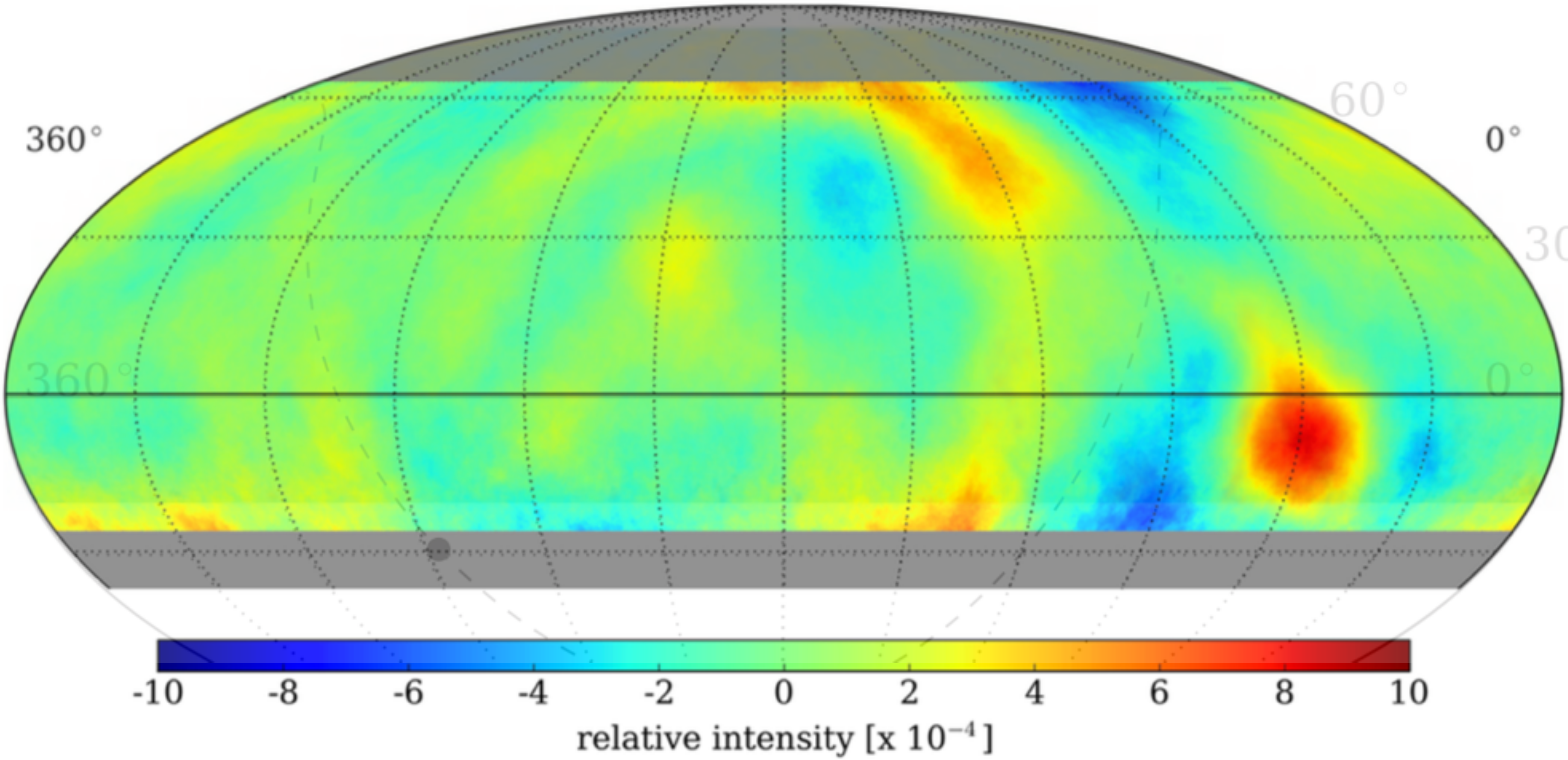

Comparing Previous Results

- Comparison to ARGO-YBJ (different smoothing)

R. Bartoli et al., Phys Rev D**88**:082001, 2013

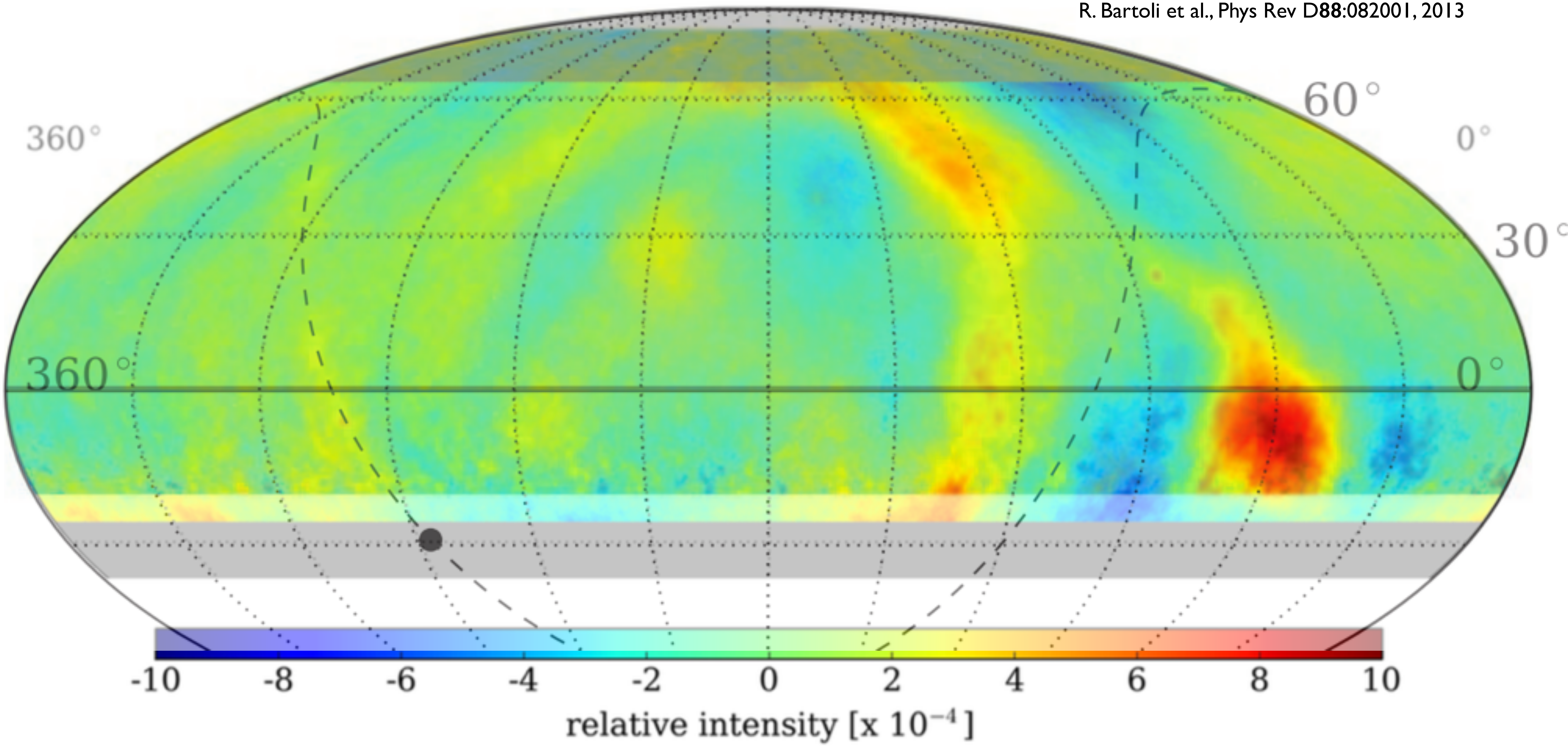

Comparing Previous Results

- Comparison to ARGO-YBJ (different smoothing)

R. Bartoli et al., Phys Rev D88:082001, 2013

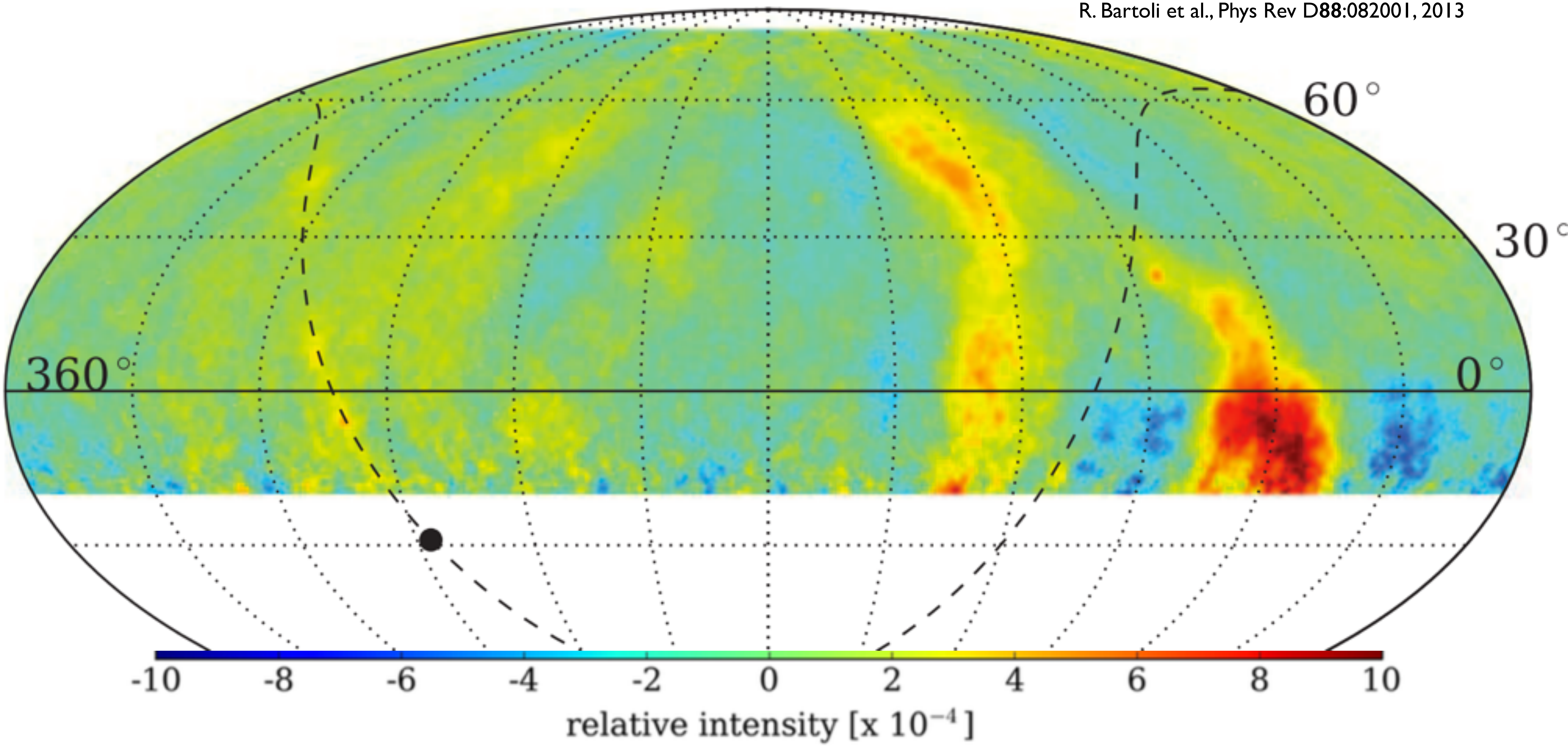

Comparing Previous Results

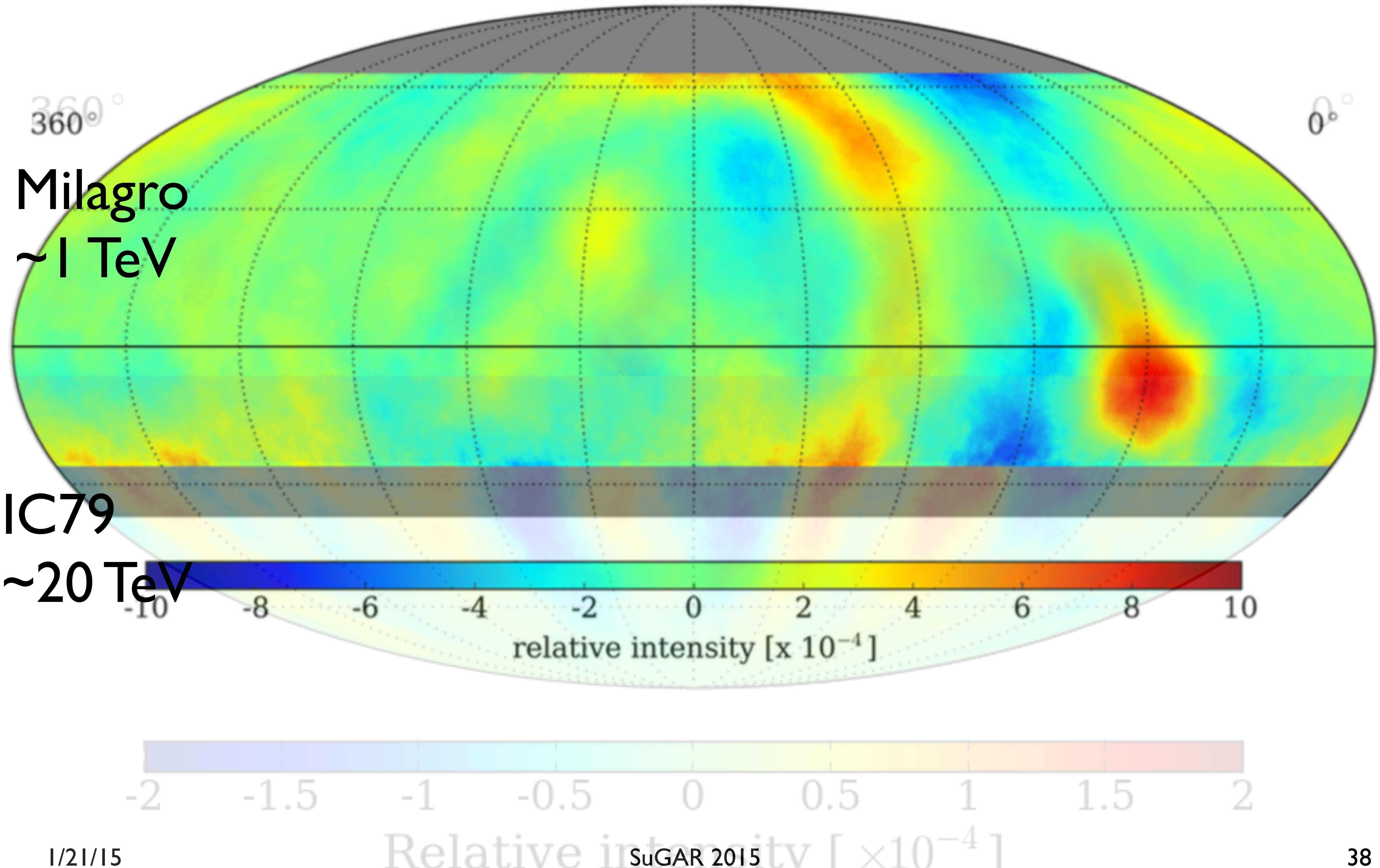

Comparing Previous Results

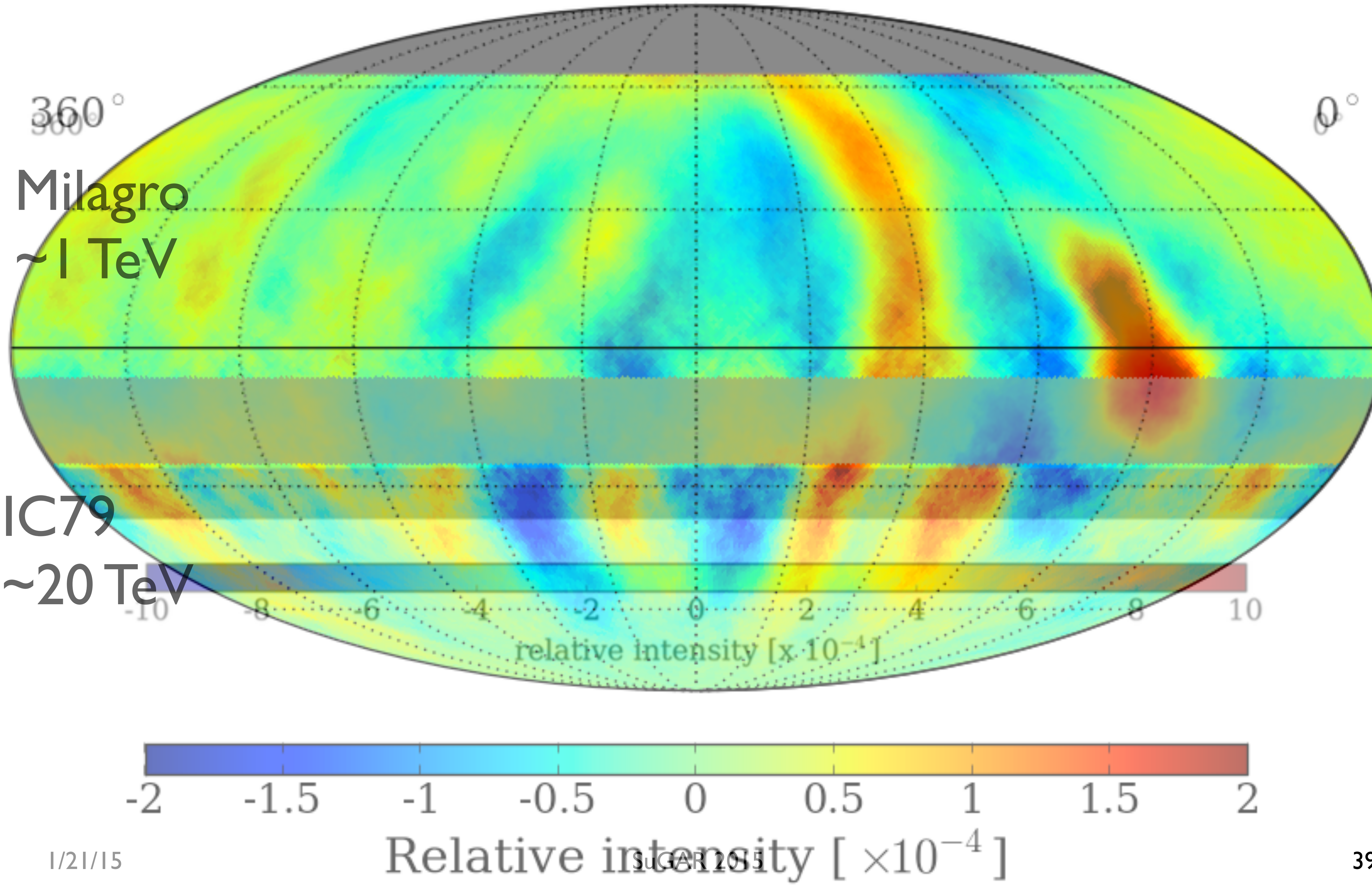

Comparing Previous Results

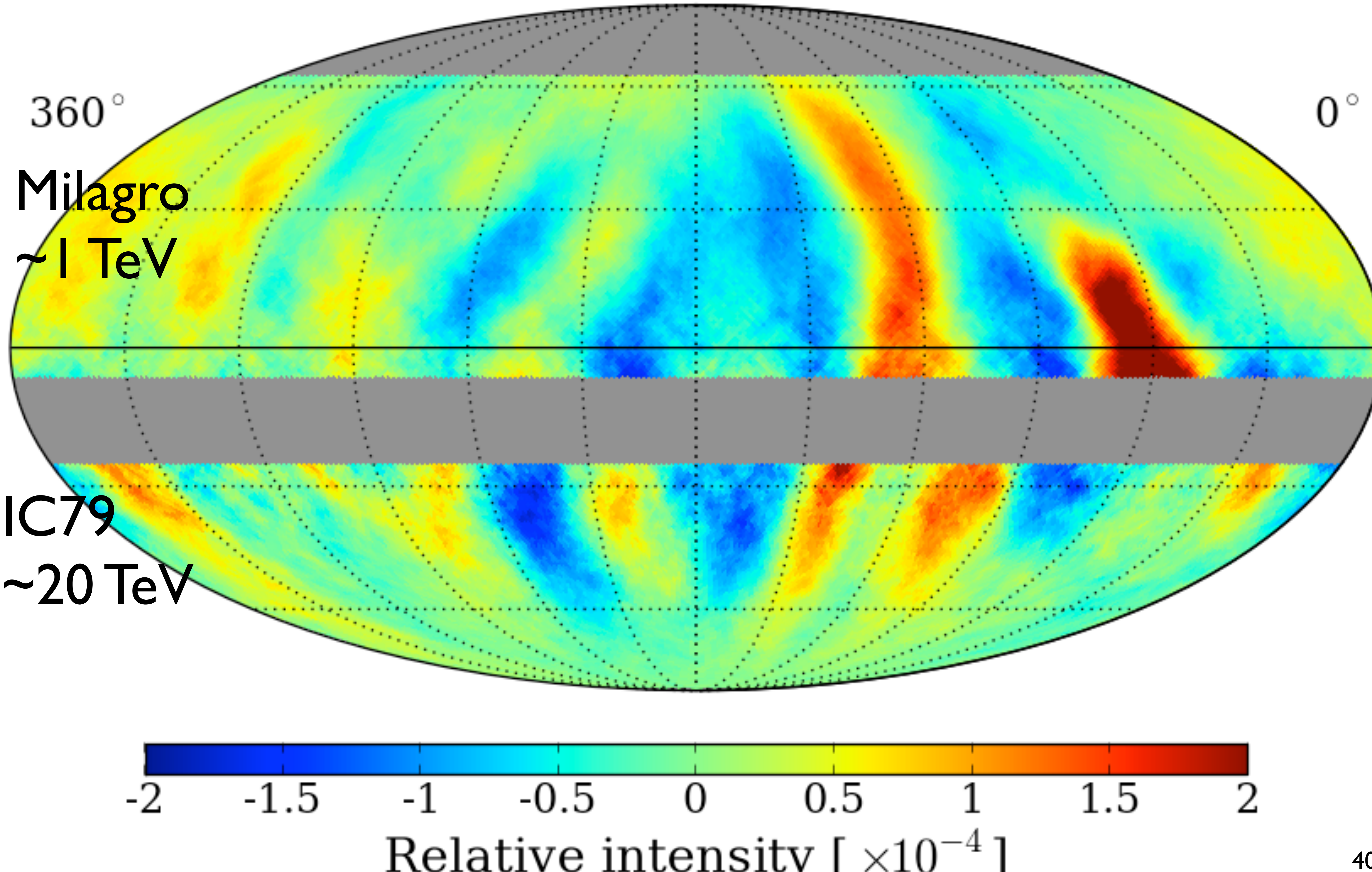

Interpretations

- Large scale anisotropy: diffusion from over-density of sources in direction of GC. <1% effect, flips in orientation (observed in data)
  - Erlykin & Wolfendale (2006), Blasi and Amato (2011), Sigl and Giacinti (2012), Streshnikova et al. (2013)
- Small scale structure (<10°):
  - Distortion of "dipole" in turbulent fields (caustics): Giacinti and Sigl (2012), Ahlers (2014)
  - Unusual interstellar magnetic field configuration: Aharonian (2008), Salvati and Sacco (2009), …
  - Heliospheric effect: Desiati and Lazarian (2013), Schwadron (2014)
  - Beyond the Standard Model: DM annihilation (Harding, 2013), strangelets (Perez-Garcia, 2014)

Summary

- HAWC-250 is up and running, final channels being deployed now and connected to DAQ
- Cosmic ray observations:
  - 20 kHz event rate (4x IC86), E_{median} = 2 TeV
  - Lunar and solar shadows observed with high significance
  - Large scale structure observed, uncorrected for known systematic effects
  - Small-scale structure appears to match previous measurements in Northern Hemisphere (with caveats)
- Up next: full year of data, LS maps, cosmic electrons

TeV Observatories

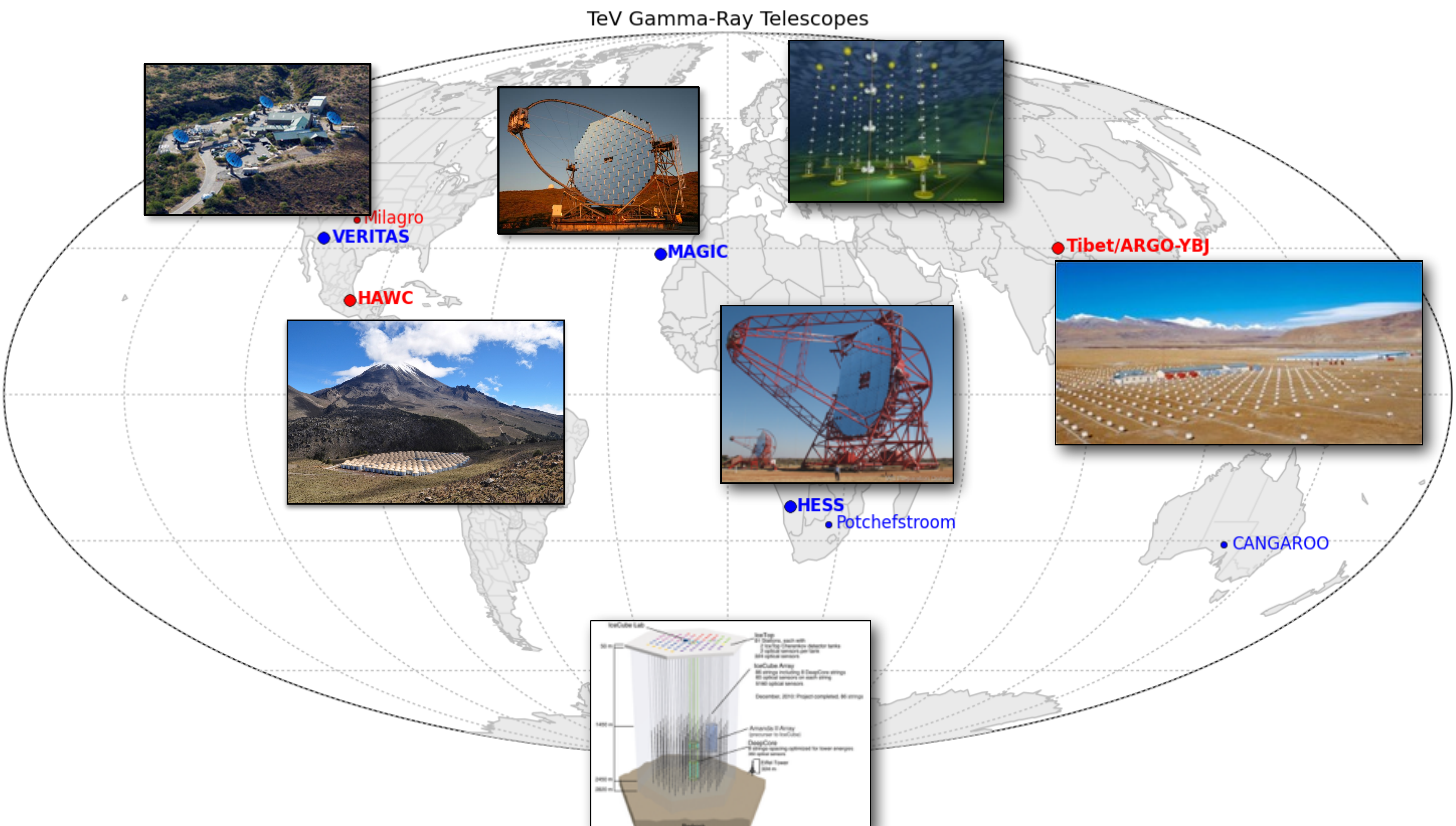

Water Delivery

Water was filtered at Esperanza and trucked to the site. 13 trips needed per tank

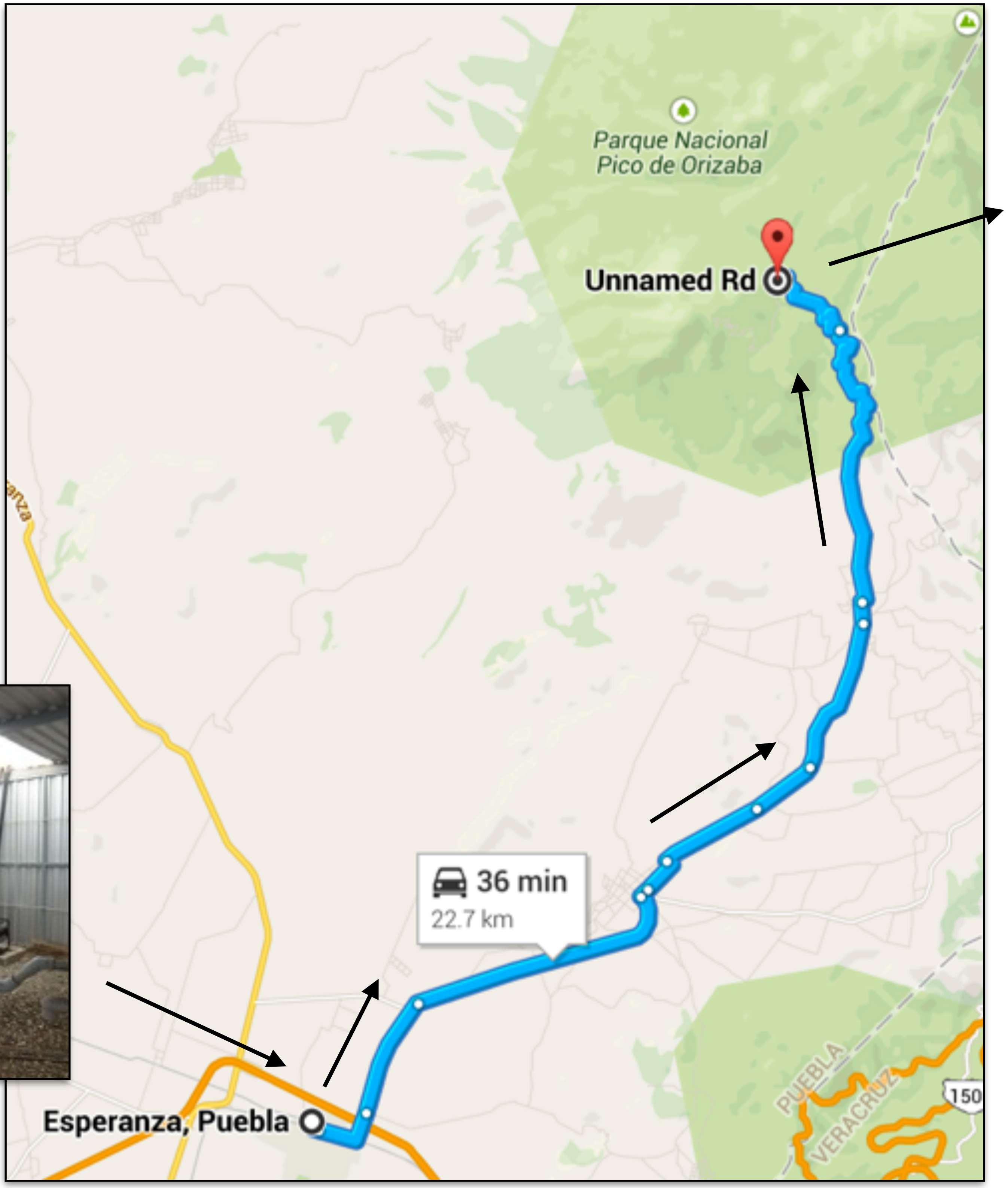

Local Geology

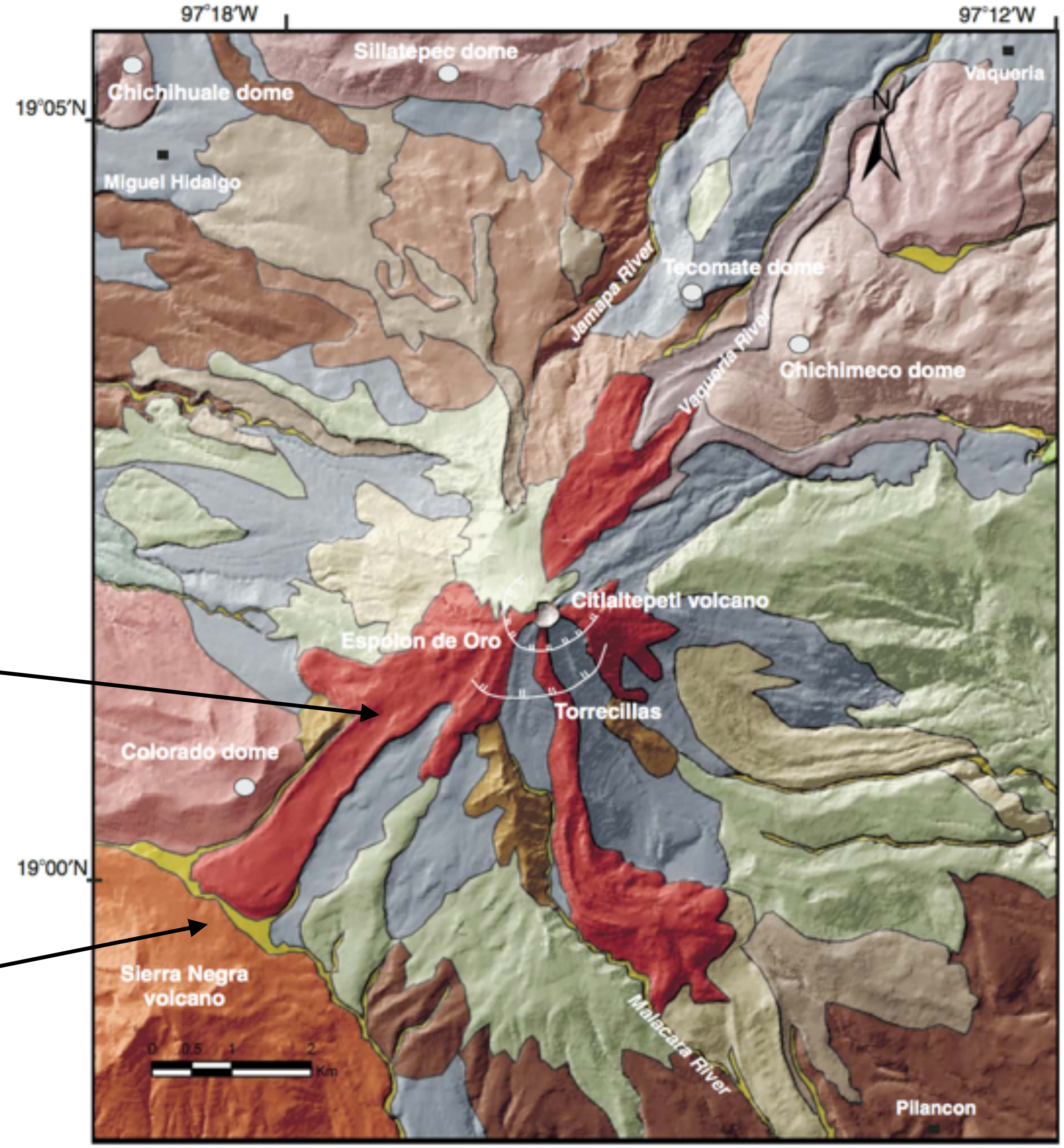

J L Macías, GSA Special Papers 422:183, 2007

Lava Flows
2100 B.C.

HAWC

Recent Eruptions:
1613, 1687, 1846

Geomagnetic Chart (2010-2015)

S. Maus et al., *The US/UK World Magnetic Model for 2010-2015*, NOAA Technical Report NESDIS/NGDC (2010)

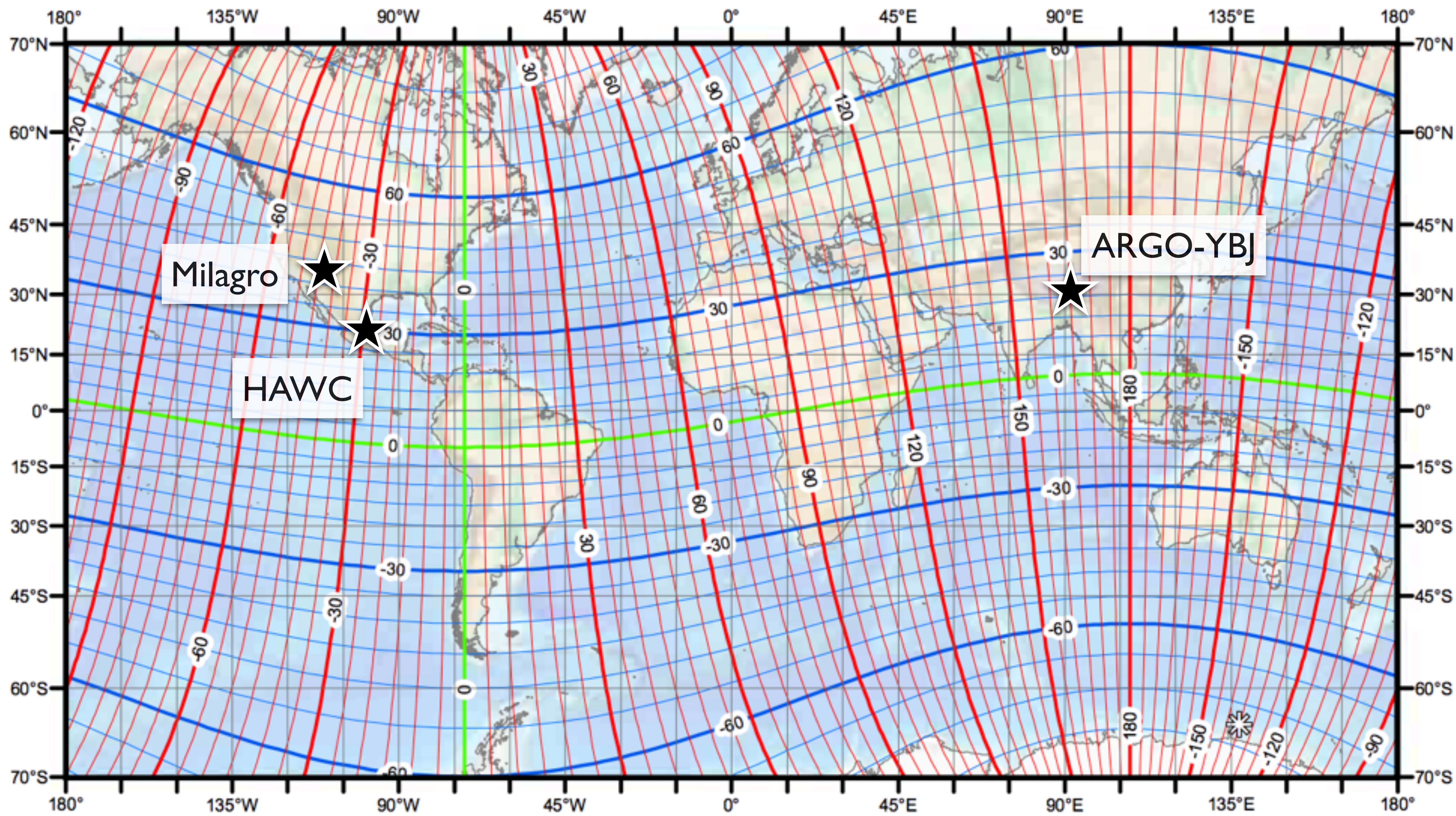

Side Effect: Map Artifacts

- Data: signal + 1000x larger background

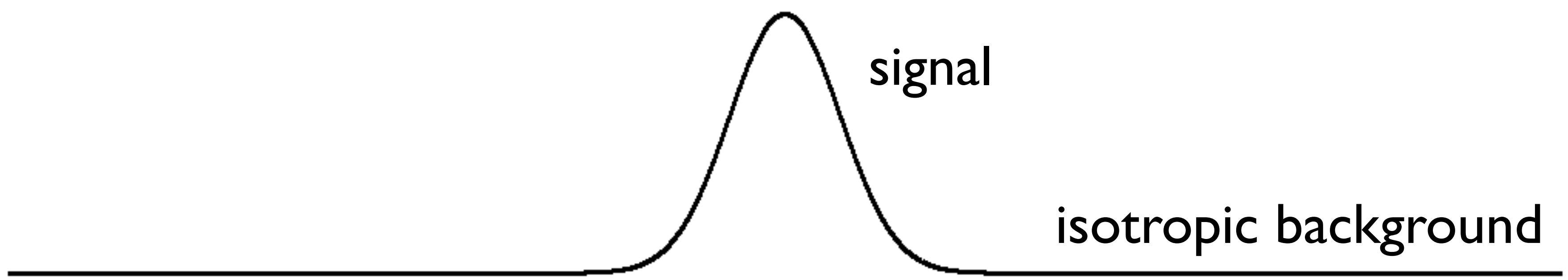

- Use data themselveses to estimate the background

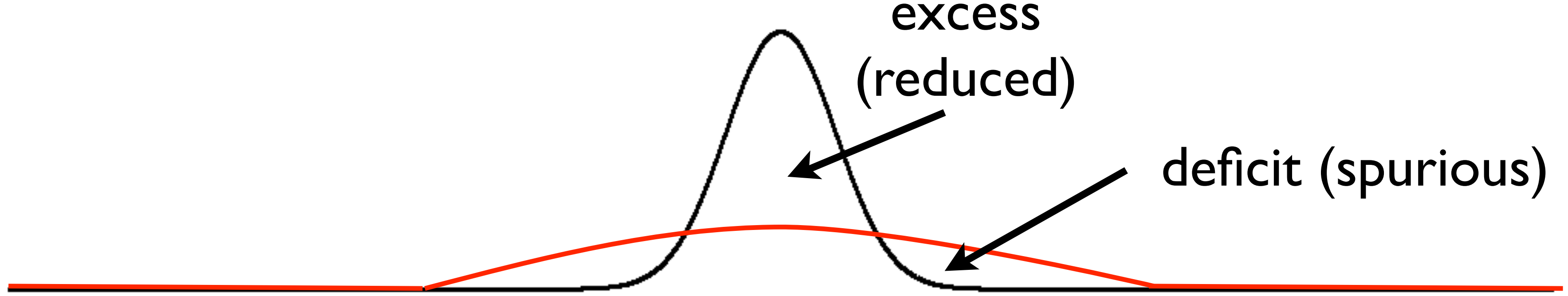

- Consequence: spurious deficits near excess regions

IceCube Power Spectrum

M. Ahlers, arXiv:1310:5712